Investigation of the Failure Modes of Concrete Dams - Physical Model Tests

Dam Safety Office

Report No. DSO-02-02
Department of the Interior
Bureau of Reclamation
May 2002

REPORT DOCUMENTATION PAGE

Form Approved
OMB No. 0704-0188

1. AGENCY USE ONLY *(Leave Blank)*	2. REPORT DATE	3. REPORT TYPE AND DATES COVERED
	May 2002	

4. TITLE AND SUBTITLE

Investigation of the Failure Mode of Concrete Dams

5. FUNDING NUMBERS

.

6. AUTHOR(S)

David W. Harris, PhD, PE

7. PERFORMING ORGANIZATION NAME(S) AND ADDRESS(ES)

Bureau of Reclamation
Denver Federal Center
P.O. Box 25007
Denver, CO 80225-0007

8. PERFORMING ORGANIZATION REPORT NUMBER

DSO-02-02

9. SPONSORING/MONITORING AGENCY NAME(S) AND ADDRESS(ES)

10. SPONSORING/MONITORING AGENCY REPORT NUMBER

11. SUPPLEMENTARY NOTES

12a. DISTRIBUTION/AVAILABILITY STATEMENT

Available from the National Technical Information Service, Operations Division, 5285 Port Royal Road, Springfield, Virginia 22161

12b. DISTRIBUTION CODE

13. ABSTRACT ***(Maximum 200 words)***

This report describes the design and testing of physical models of concrete arch dams. Two series of models are included. In the first series, a planar, two-dimensional model which represents a 1/50 scale model of the Koyna Dam in India is tested. The model is tested without water behind the dam to utilize conditions as simple as possible for comparison with numerical modeling. Cracks formed in the test are similar to cracks which resulted on the Koyna Dam following an actual earthquake event.

The second series of models are approximately 1/150 scale of a typical wide canyon dam. Material properties are adjusted to the model scale, a reservoir and foundation are included. The models utilize different joint patterns of a monolith, single horizontal and vertical joints, and multiple vertical and horizontal joints. Models are tested to collapse of the structure. Conclusions are that initial cracking of the structure is not influenced by the joints. Final collapse is a push through of sections of the dam downstream and is controlled by the joints both with the pattern of the failure and with the acceleration required to fail the structure. Water is observed as passing through the model during the loading.

14. SUBJECT TERMS

concrete dam, earthquake, physical model, arch dam, failure, Koyna Dam, gravity dam, dynamic testing

15. NUMBER OF PAGES

50

16. PRICE CODE

17. SECURITY CLASSIFICATION OF REPORT	18. SECURITY CLASSIFICATION OF THIS PAGE	19. SECURITY CLASSIFICATION OF ABSTRACT	20. LIMITATION OF ABSTRACT
UC	UC	UC	UC

Investigation of the Failure Modes of Concrete Dams - Physical Model Tests

DSO-02-02

by Dave W. Harris, PhD, PE
Materials Engineering and Research Laboratory Group

May 2002

Acknowledgments

This research was sponsored by the Dam Safety Program of the U.S. Bureau of Reclamation

Contents

Tables

Figures

Page

Introduction

One of the most studied cases of a dam subjected to earthquake loading is the Koyna Dam in India. This 338-foot (103-meter) high dam suffered cracking during a magnitude 6.5 earthquake in 1967.[1] During this event, the ground acceleration in the stream direction reached 0.49 g, with a total duration of strong shaking that lasted about 4 seconds. At the time of the event, the reservoir elevation was 37 feet below the crest.

Following the Northridge Earthquake in California (January 17, 1994) and the Kobe Earthquake in Japan (1 year later, on January 17, 1995), greater consideration is being given to the magnitude of the vertical acceleration of seismic events. Continuing concerns about the performance of concrete dams subjected to severe earthquakes has motivated investigation into ways to analyze and predict this performance using nonlinear numerical analysis techniques.[2] In some cases, linear dynamic analyses indicate high stresses that can be further studied only with nonlinear models.

Two-Dimensional Koyna Dam Cross Section Test

Background

Previous studies of the behavior of concrete dams subjected to seismic accelerations have been conducted on single gravity dam monoliths.[2,3,4,5] In references 2 and 3, attention was given to developing a modeling material that maintained similitude with the prototype. In reference 2, the authors compared models to linear elastic analysis results. More recent studies[6,7] have compared scaled centrifuge models to numerical models.

The purpose of this investigation, conducted at the Bureau of Reclamation, Materials Engineering and Research Laboratory, was to produce laboratory results for comparison to nonlinear computer models. The geometry of the model was scaled from the Koyna Dam and follows previous work.[2,3] Because numerical models that predict failure were to be compared, models were formulated that ,to the extent possible, maintained similitude relationships and yet were simple enough for direct comparison with computer-predicted results. To this end, unlike previous studies,[2,3] similitude with reservoir effects was not attempted. This eliminated the need to model coupling effects. Two models were tested: a model with a natural but preexisting crack and a continuous model cracked during testing.

Physical Model Test

The scale chosen for this model was 1/50. Similitude requirements for models have been summarized in other references,[8] and estimated properties of Koyna Dam have also been suggested.[2,3] These properties are summarized in table 1.

Table 1.—Estimated concrete properties, the associated scale factors, and the model material target values

Property	Prototype estimate	Scale factor	Target value
E	4,000,000 lb/in^2 (27,940,000 kN/m^2)	50	80,000 lb/in^2 (558,800 kN/m^2)
f_c'	4,000 lb/in^2 (27,940 kN/m^2)	50	80 lb/in^2 (558 kN/m^2)
f_t	400 lb/in^2 (2,794 kN/m^2)	50	8 lb/in^2 (55.9 kN/m^2)
Density	150 lb/ft^3	1	150 lb/ft^3
ε_u^c	0.0025	1	0.0025
ε_u^t	0.00012	1	0.00012

Concrete Mix Design and Material Properties

In this study, a new, low-strength concrete mix was designed. Considerable work has been done in previous studies[2,3,9] to produce a similitude-appropriate concrete mix. As has been suggested, curing and the associated shrinkage cracking can be problematic in the use of concrete mixes with highly reduced properties. In addition, the use of any lead product to meet density requirements poses special problems for the handling, storage, and disposal of this hazardous substance. This latter problem, in particular, limits the options for commercial mass production of the material and complicates he disposal of it. When modeling nonlinear failures, additional consideration must be given to ensuring that the correct failure mechanism is reproduced at model scale.

The mix for this study used bentonite pellets as a component to reduce strength. The use of bentonite pellets posed a logistic problem because saturation of the bentonite is required before mixing. The mix components and proportions for the initial laboratory mixed concrete and the commercially mixed model concrete are shown in table 2.

Table 2.—Model concrete mix components

Component	Lab mix (lb/yd^3)	Volume in mix (ft^3)	Model mix (lb/yd^3)	Volume in mix (ft^3)
Air		0.14 (1/2% entrapped air assumed)		0.52 (1/2% entrapped air assumed)
Water	560	8.99	480	7.68
Cement	160	0.82	168	0.86
Bentonite	40	0.25	42	0.26
Sand	1,366	8.4	1,454	8.87
No. 4 - 3/8" gravel	553	3.36		
3/8" - 3/4" gravel	829	5.04	1,458	8.81
Note: water/cement = 3.5 Bentonite/(Bentonite+Cement) = 20%				

The trial mix was initially made in the laboratory, and bentonite saturation was accomplished overnight. Based on the apparent success of this mix, both shake table models were made using this design. Because of the volume required for a shake table model (6 yd^3), the actual model mix was supplied commercially. For the commercially supplied concrete, it was assumed that saturation would take place in the mixer drum during transit. Water was adjusted from the original design at the plant to decrease sloshing in transit. Onsite, a slump of approximately 7.5 inches was used as an indicator of a correct mix. The slump was not a good indicator of strength, as indicated by changes in the properties of the concrete. Results from the two mixes are shown in table 3.

Breaks for all compressive cylinder tests demonstrated in a classic shear plane typical of concrete of approximately 65 degrees. Other materials were tested in the lab, based on lead/plaster combinations as trial mixes. These materials created failure modes not typical of concrete, such as horizontal layer crushing. It is clear that not all parameters matched the similitude requirements simultaneously. Changes in mix water had the largest effect on strength. However, as was stated previously, the primary intent was to produce calibration data for testing of computer models.

Laboratory testing was performed in support of the tests, and standard tests were run. Typical static compression stress-strain data is shown in figure 1. Specialized tests were used to help assist in the calculation of parameters that may be required in nonlinear computer material models. Typical fracture (crack width versus load-beam test) data are shown in figure 2, and unload-reload data demonstrating plasticity of the material are shown in figure 3. These tests were not intended to be an exhaustive set of all tests required for published numerical models, but are believed to be representative of the types of data needed.

Table 3.—Properties of model materials

Property	Lab trial results	Apparent scale (dimensional scale target)	Model mix—Koyna I	Apparent scale (dimensional scale target)	Model mix—Koyna II	Apparent scale (dimensional scale target)
Density (lb/ft^3)	133.1	0.9 (1.0)	135	0.9 (1.0)		
E (lb/in^2)						
7 days			42,000	89 (50)		
15 days					157,000	25 (50)
28 days	74,000	54 (50) (Density corrected by E = scale*density = 50)[6]	55,000	72 (50)		
Rapid loading						
15 days					113,000	
28 days	93,457					
35 days			80,000			
f_c'						
Static loading						
7 days	50	80 (50)	89 (50)	45 (50)		
15 days					203	20 (50)
28 days	84	48 (50)	154 (50)	26 (50)		
120 days			290			
Rapid loading						
7 days	70					

Table 3.—Properties of model materials (continued)

Property	Lab trial results	Apparent scale (dimensional scale target)	Model mix—Koyna I	Apparent scale (dimensional scale target)	Model mix—Koyna II	Apparent scale (dimensional scale target)
f_t						
Static						
15 days/split tension					27	15 (50)
15 days/beam tension					60	
21 days/direct tension			14	29 (50)		
21 days/beam tension			32			
28 days/split cylinder	12	33 (50)	20	20 (50)		
28 days/beam tension			49			
Rapid loading						
15 days/split cylinder					52	8 (50)
28 days/split cylinder	22					
$\varepsilon_u{}^c$	0.004	2 (1)	0.005	2.5 (1)	0.004	2 (1)

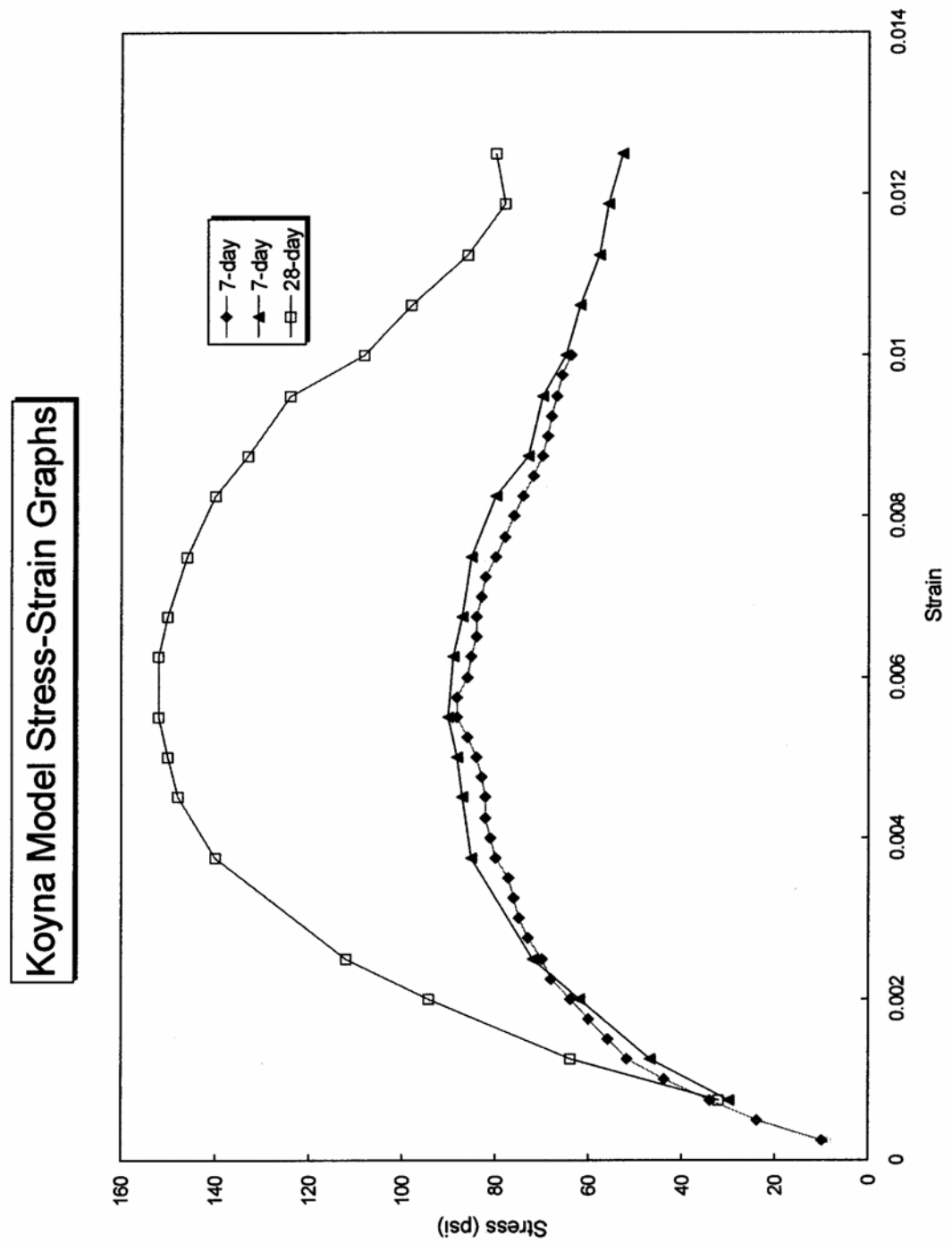

Figure 1.—Stress-strain graphs.

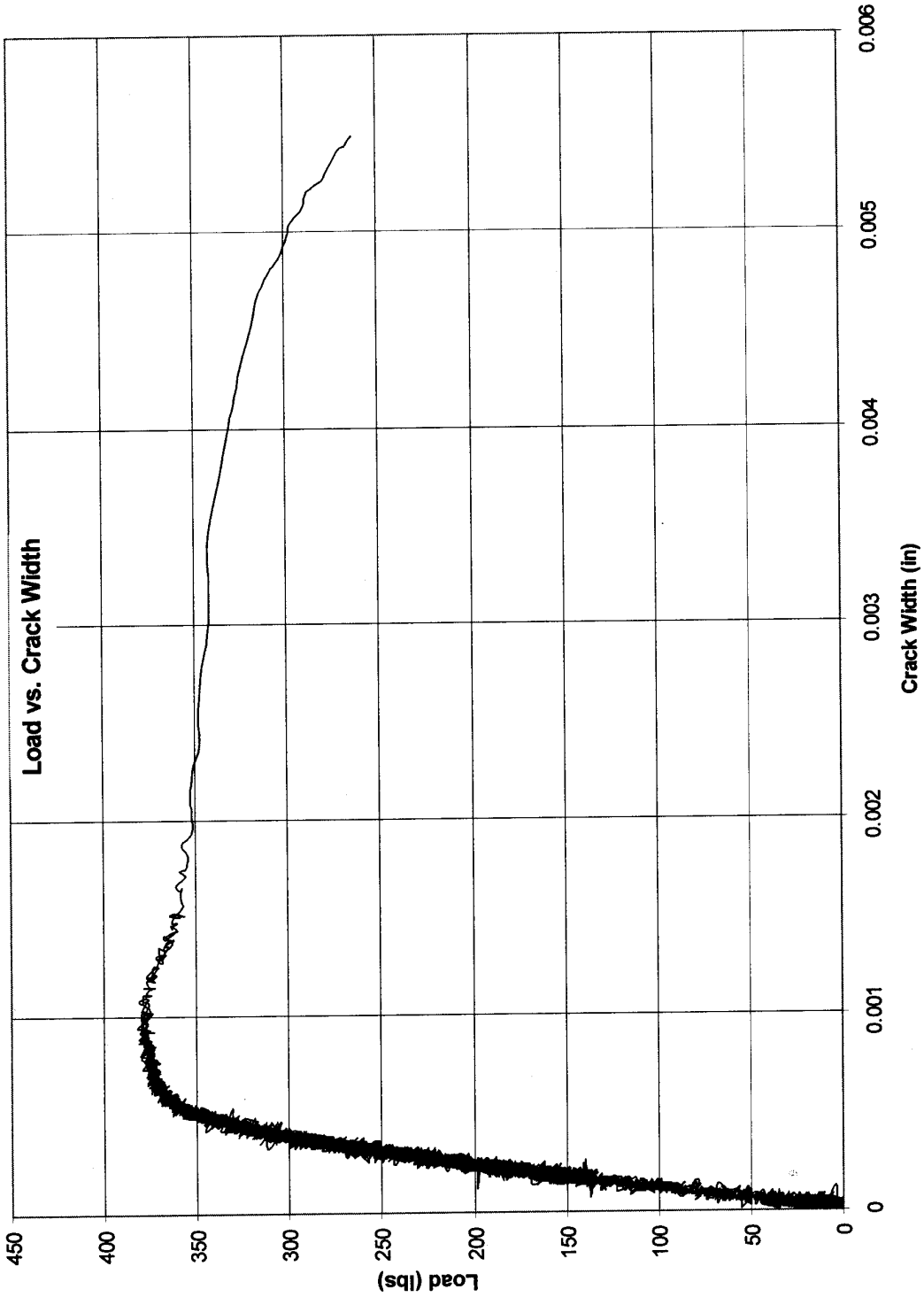

Figure 2.—Load versus crack width in beam tension.

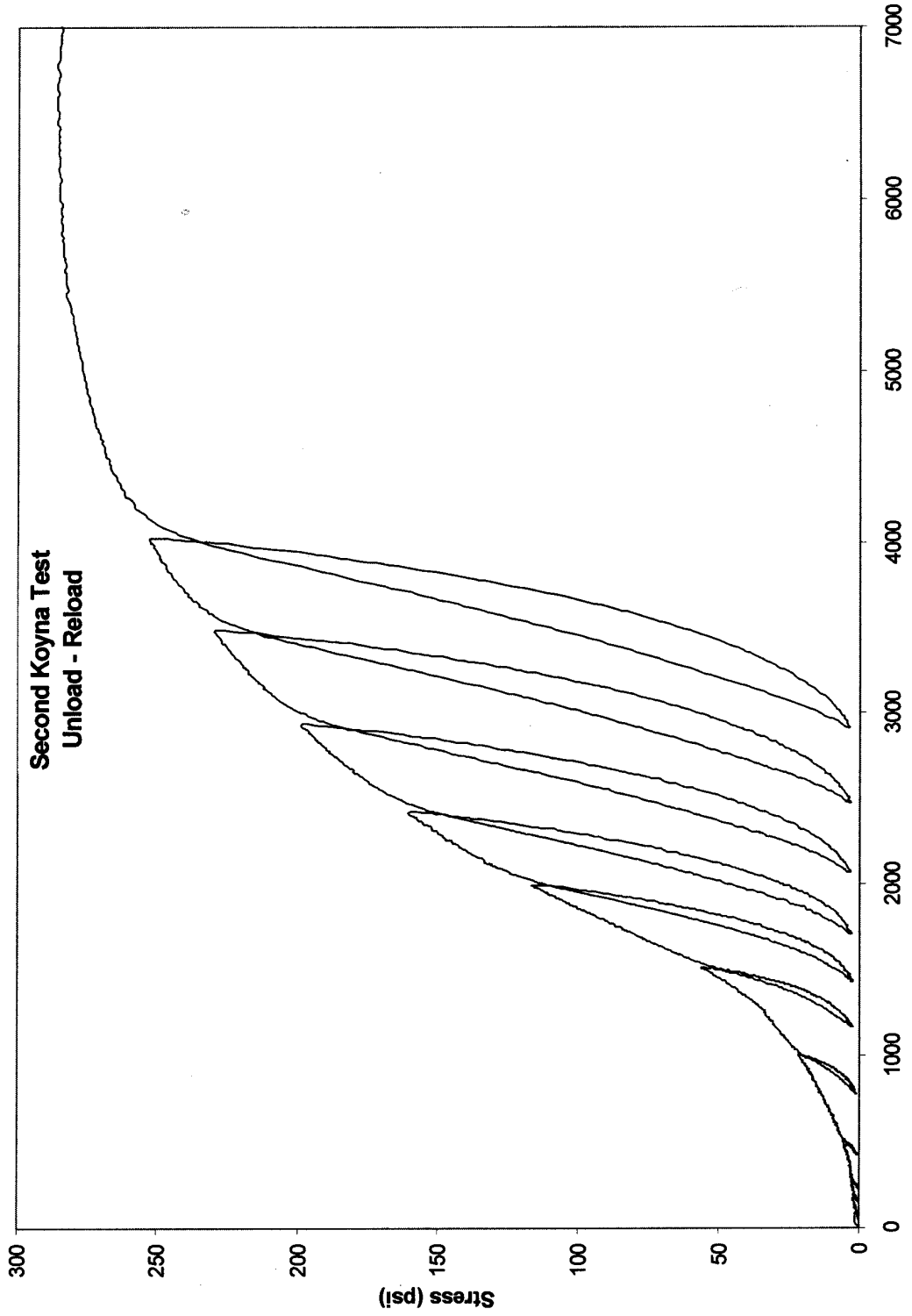

Figure 3.—Unload-reload test, showing plastic behavior of the low-strength concrete.

Model Construction and Instrumentation

The tests were performed in the U.S. Bureau of Reclamation, Materials Engineering and Research Laboratory. The Vibration Laboratory is used for large-scale tests and has been in existence at Reclamation since 1969.[10] For these experiments, a shake table was constructed that has movement constrained to a single axis (horizontal only). The table was tested for its response modes and also tested in motion with accelerometers to determine its capabilities for use at higher frequencies. The table responded well for input frequencies below 22 Hz, which was below the table's lowest natural frequency of 30 Hz, but higher frequencies were eliminated from testing. Response of the table was clearly best at frequencies of 26 Hz and below. For this reason, a similitude simulation of an earthquake motion was not used. Rather, for practical reasons associated with the table and for simplicity in numerical model calibration, a sinusoidal motion was selected.

In figure 5, the model is shown on the shake table. The 1/50 scale model resulted in an 8.5-foot-tall model weighing 7,850 pounds. A slab, representing a foundation, was cast monolithically with the model to provide a fixed lower boundary at the base of the dam. Instrumentation measured displacements and accelerations of the model and input motion of the actuator. The general instrumentation locations are shown in figure 6 and table 4.

The first model was cast lying on its side. In this position, form construction and concrete placement were much easier, access was provided to an entire face, and the depth of material was only 1 foot 9 inches. After a period of approximately 20 days, a small shrinkage crack appeared in the exposed face. At this time, tension tests that may be useful in modeling the onset of shrinkage were run. At approximately 28 days, the model was positioned on the shake table and the forms were removed. The shrinkage crack was evident on the side and the sloped face of the model, and the crack was assumed to extend through the entire model. The plane of the crack had an inclination of approximately 20 degrees from horizontal toward the side of the model. After approximately 1 additional week, the surface had dried sufficiently to apply instrumentation, and the test was run.

The second model was cast upright on the shake table to avoid the shrinkage cracking experienced in the first model. By testing sooner, the onset of shrinkage cracking was avoided, and the second model produced a material failure under dynamic loading. Testing earlier also held the curing strengths lower. Laboratory testing was performed on test specimens of the same material immediately following the breaking of the model.

Input Motions

Numerical analysis predicted that the frequency of the fundamental mode of the model was approximately 14 Hz, but this fundamental mode was out of the plane of the test (i.e., side to side in the two-dimensional model. The cantilever mode, mode 2 of the model but the first mode in the plane of the test, was predicted at approximately 28 Hz. Modal sweeps were run on the model at frequencies starting at 2 Hz and increasing to 28 Hz, with a constant input acceleration

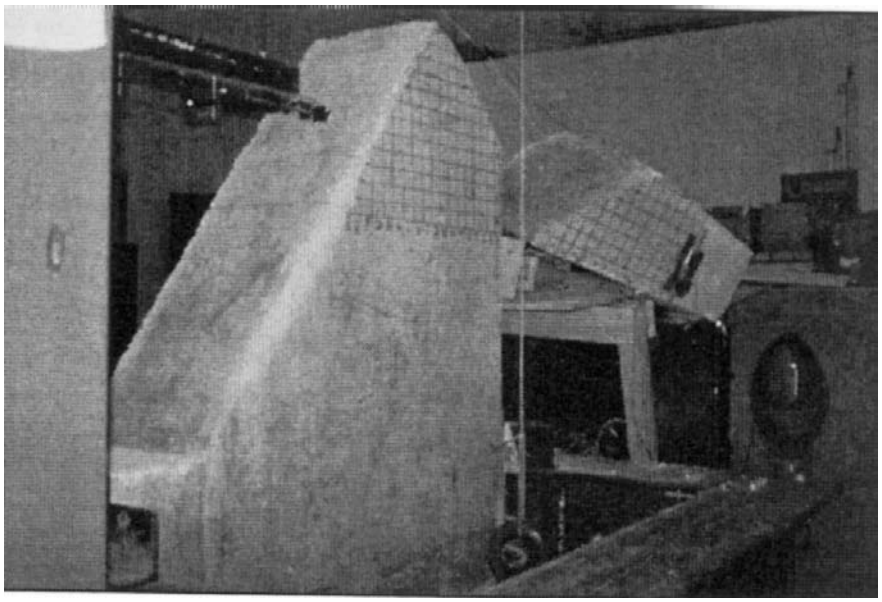

Figure 4.—Second Koyna model failure plane.

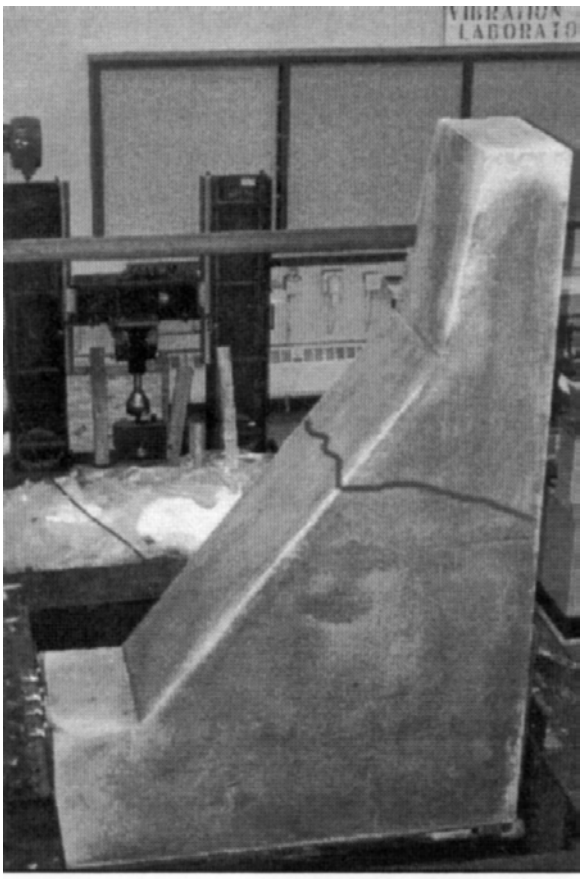

Figure 5.—First Koyna model mounted on the shake table. The shrinkage crack and eventual failure plane is sketched in.

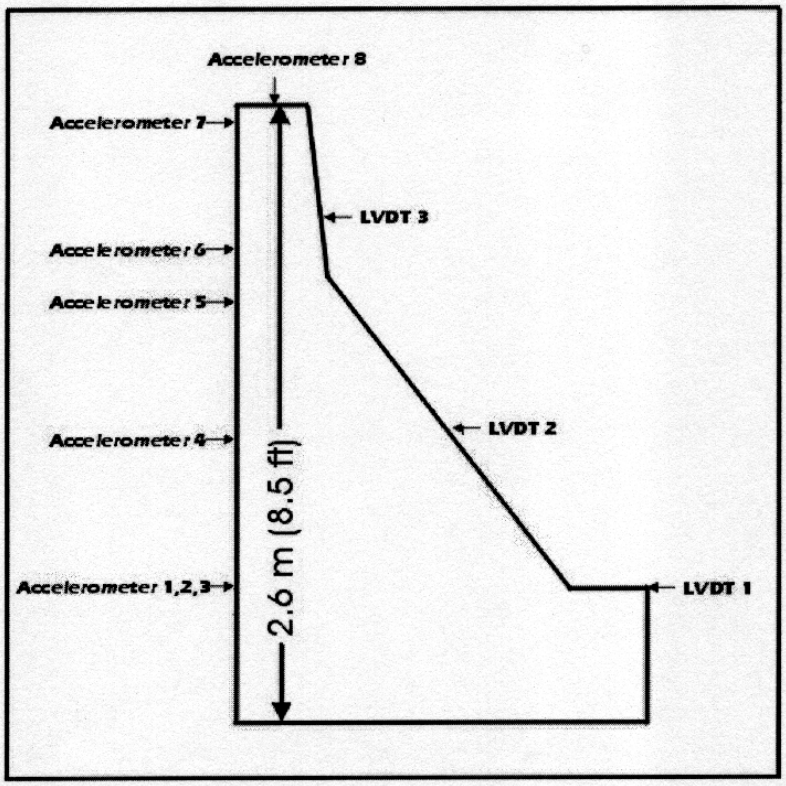

Figure 6 – Instrument Locations

Table 6: **Instrumen**
Locations

INSTRUMENT ID	TYPE	ORIENTATION	HEIGHT FROM BASE
Accelerometer 1	Acceleration	Horizontal, x-direction	0
Accelerometer 2	Acceleration	Horizontal, y-direction	0
Accelerometer 3	Acceleration	Vertical	0
Accelerometer 4	Acceleration	Horizontal, x-direction	0.66 m (2.17 ft)
Accelerometer 5	Acceleration	Horizontal, x-direction	1.22 m (4.00 ft)
Accelerometer 6	Acceleration	Horizontal, x-direction	1.47 m (4.83 ft)
Accelerometer 7	Acceleration	Horizontal, x-direction	2.03 m (6.67 ft)
Accelerometer 8	Acceleration	Vertical	2.03 m (6.67 ft)
LVDT 1	Displacement	Horizontal, x-direction	0
LVDT 2	Displacement	Horizontal, x-direction	0.97 m (3.17 ft)
LVDT 3	Displacement	Horizontal, x-direction	1.69 m (5.54 ft)

of 0.1 g. The results are shown in figure 7. The first input frequency that showed an increase of acceleration above the input was 14 Hz. The effect was demonstrated in the plane of testing. Higher frequencies produced a more dramatic effect. A sinusoidal motion of 14 Hz (approximately 2-Hz prototype) was chosen for the input for all subsequent calibration tests because this lowest response frequency was believed to be the easiest for numerical simulation and calibration. The earthquake record for upstream/downstream motion of the Koyna event (see figure 8) is believed to have a primary component at 2.4 Hz. This is more readily seen in the response spectrum of figure 9. With this set frequency of 14 Hz, accelerations were increased in a single horizontal direction (upstream and downstream to the model) until failure occurred.

Test Results

As mentioned above in the discussion of the input motion, the chosen input motion for the model was a 14-Hz sinusoid.

Model 1—Cracked Model

Four typical acceleration plots are shown in figures 10 through 13 for Model 1. In figure 10, the acceleration of the base of the dam and the acceleration at the base of the known crack were measured to be 0.5 g, while the acceleration of the crest of the model measured nearly 2 g. This magnification of acceleration, with height from the base of approximately 4 times, is similar to tests reported in the literature.[2,11] Neither the model nor the field case showed failure characteristics at this acceleration.

Because this model was to be used with computer programs to model sliding failure mechanisms, testing was continued. Base accelerations were increased while maintaining the 14-Hz input motion. From this point, the constant input frequency has the advantage of seeing changes in response as model characteristics change. At about a 2-g acceleration at the base, a puffing of material from the crack was observed. This was caused by a rocking motion of the top piece of the model (the block above the crack), which acted as a bellows, blowing worn material from the cracked surface.

The next increment in acceleration, at a base acceleration of 2.25 g, showed a change in response of the portion of the dam above the crack. As can be seen in figure 11, the magnification of acceleration from base to top increases, showing a maximum of 3.75 g or a magnification factor of 1.6 times. There is evidence of a phase shift of motion between the top and bottom at this time in the testing.

The next ramp of acceleration was to an acceleration of 2.5 g of the base. As can be seen in figure 12, with this acceleration, the top and bottom of the model show nearly equal acceleration, with a full 180-degree phase shift between the pieces. As can be seen in figure 14, which shows displacement at the top of the model, the top of the dam is sliding along the base by this time.

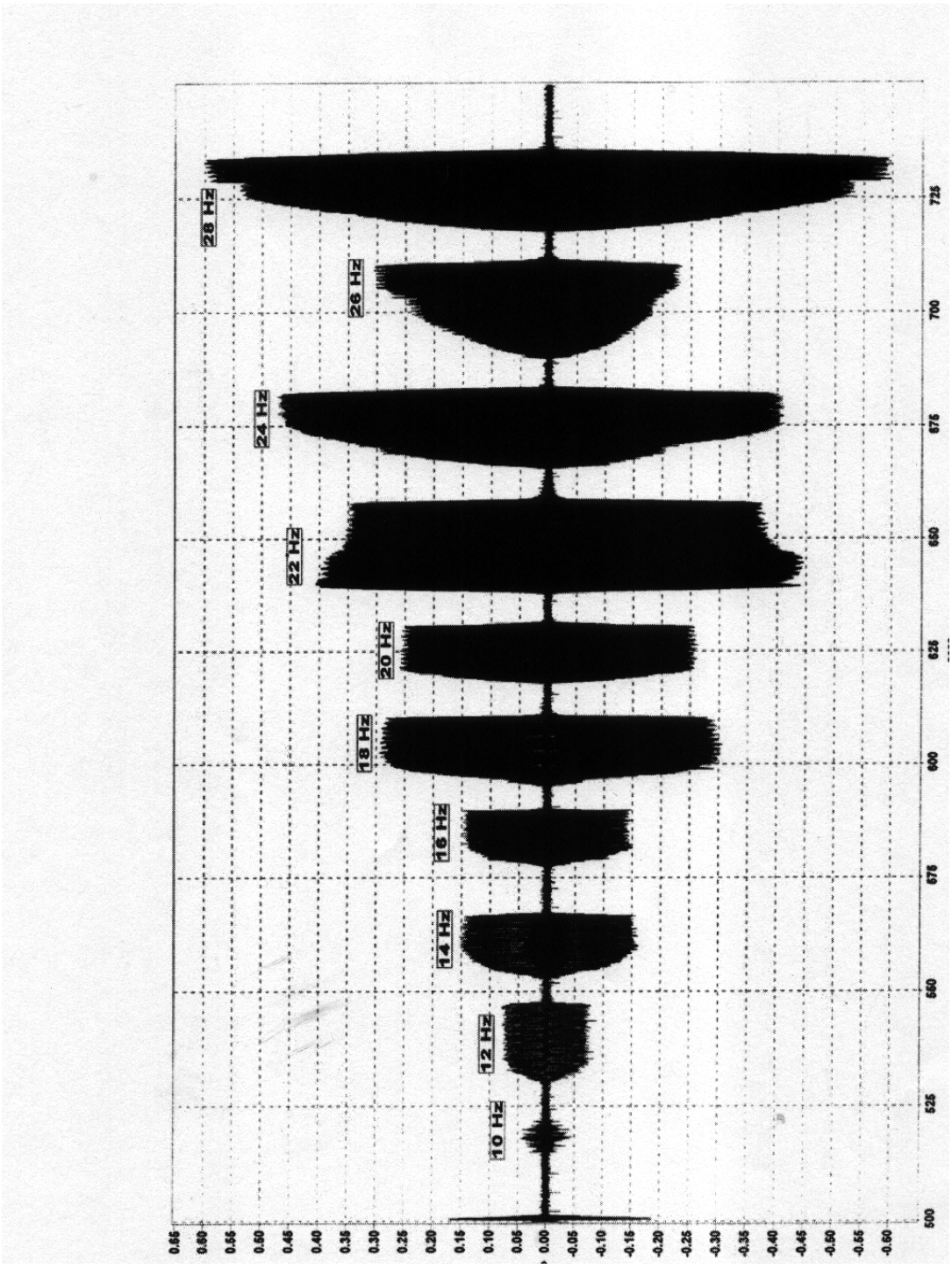

Figure 7.—First Koyna test: horizontal acceleration at the top of the model.

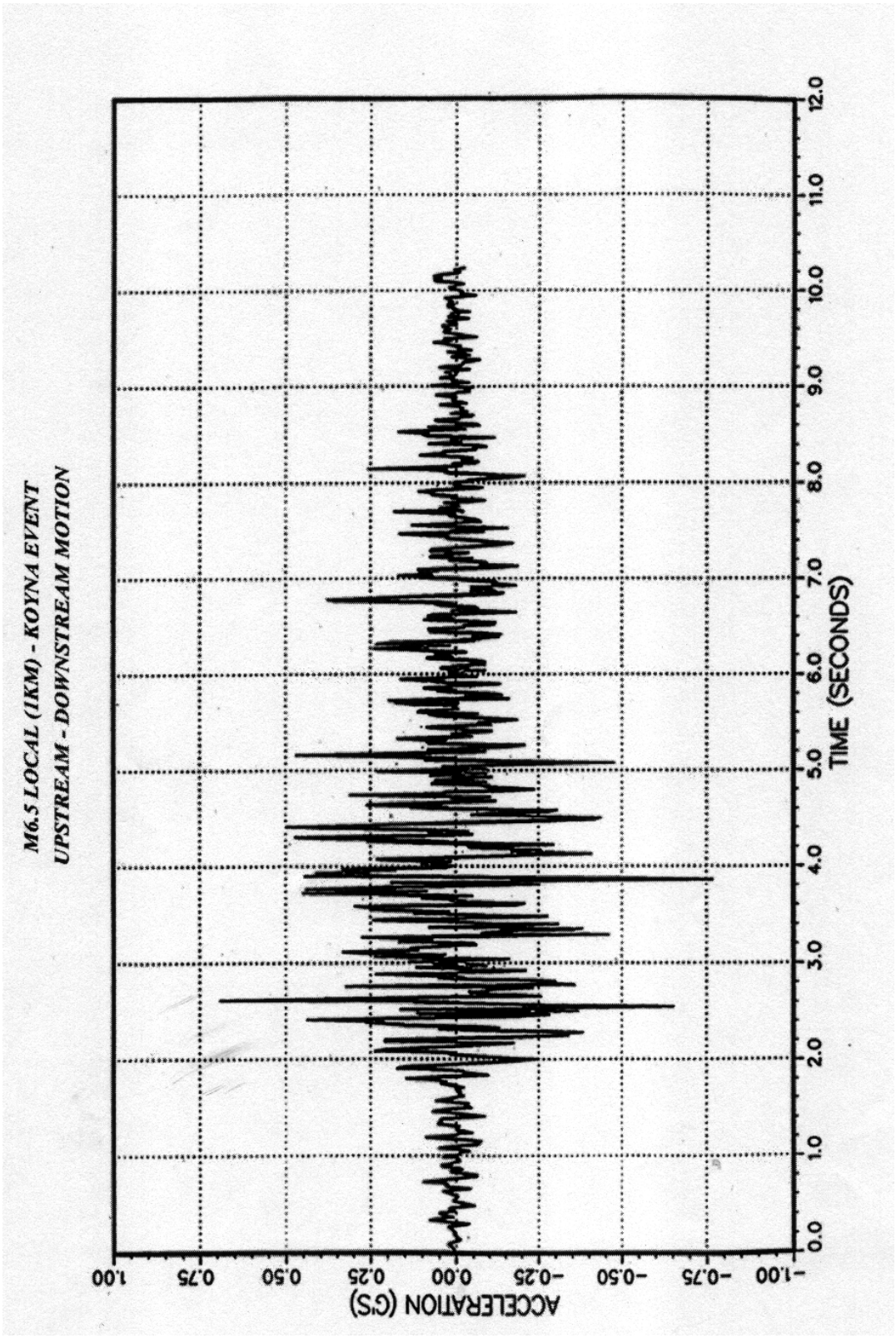

Figure 8.—The seismic record for upstream/downstream motion during the Koyna event.

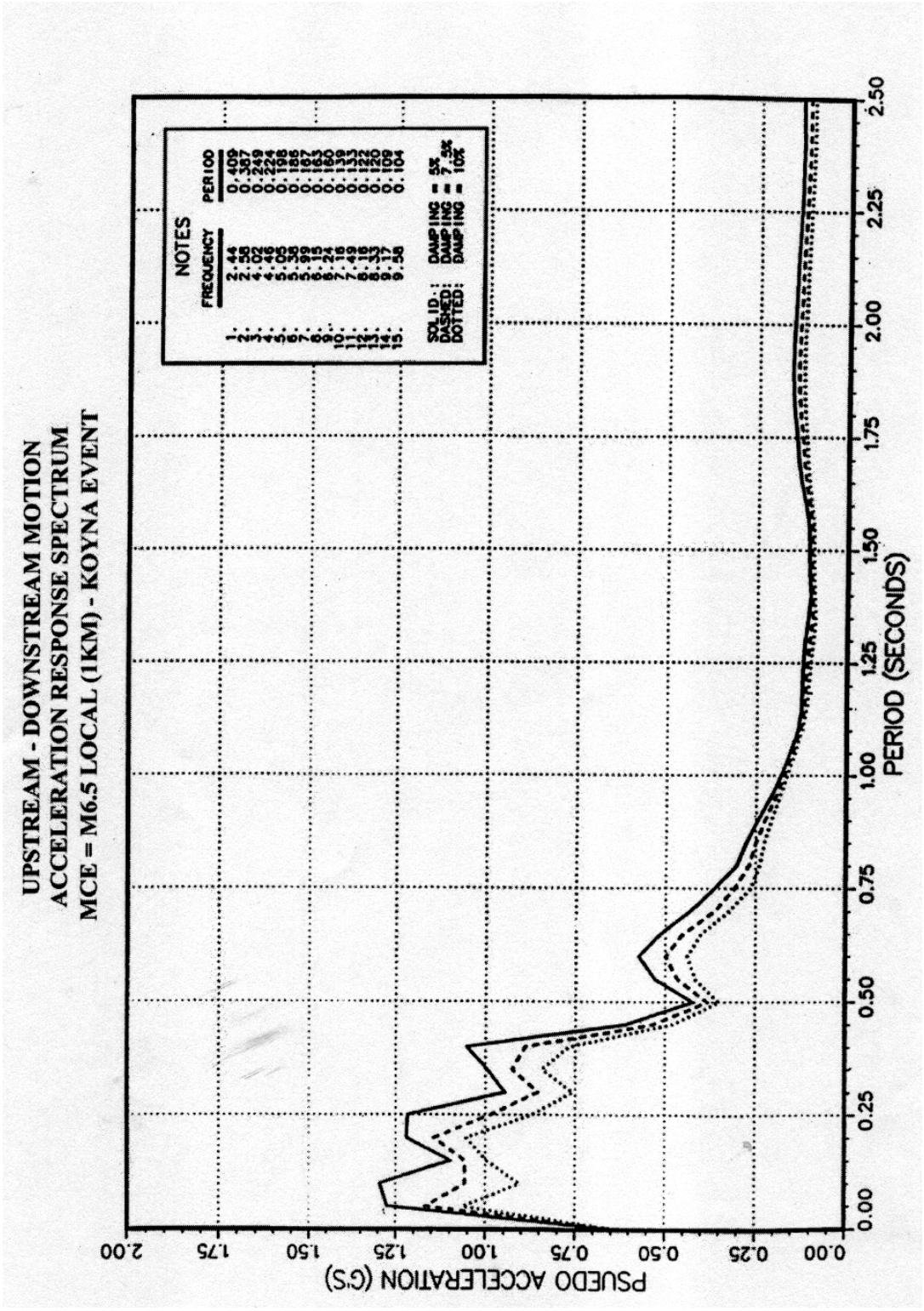

Figure 9.—Koyna response spectrum.

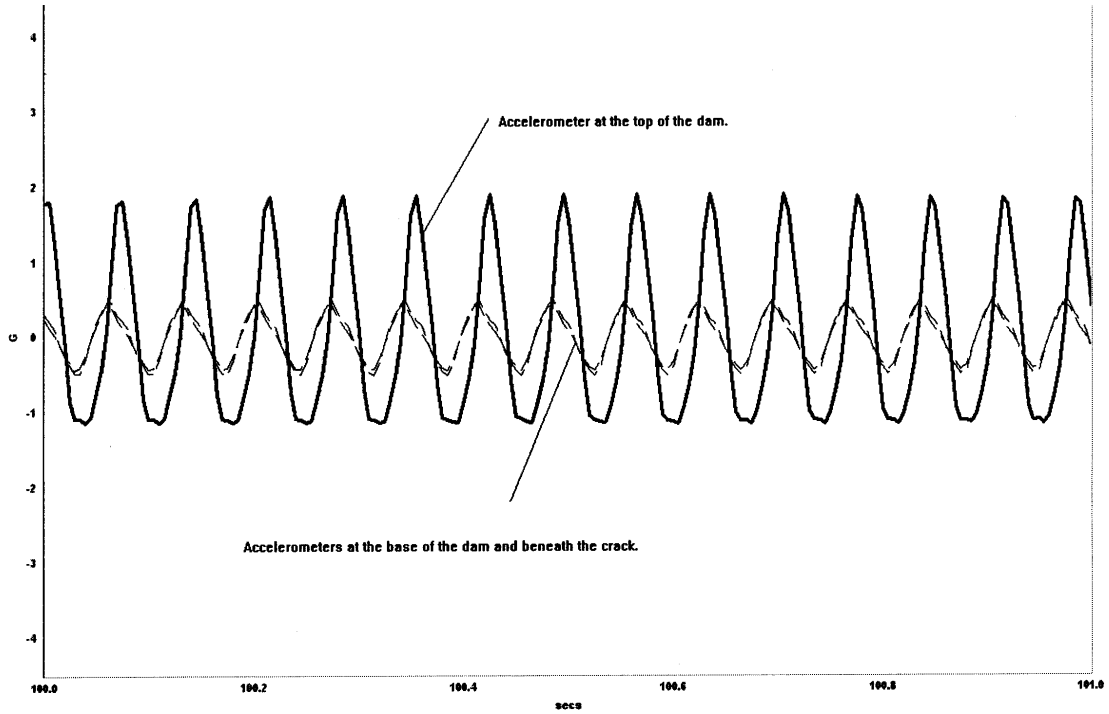

Figure 10 – First Koyna Model: Base acceleration of 0.5g.

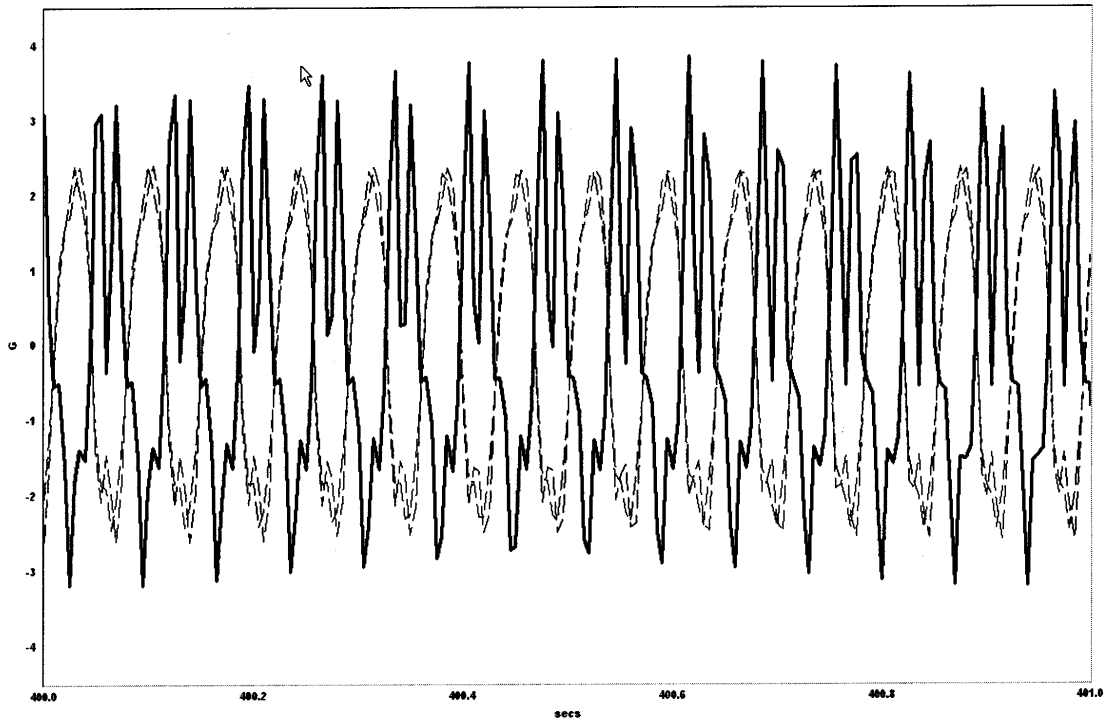

Figure 11 – First Koyna Model: Base acceleration of 2.25g's.

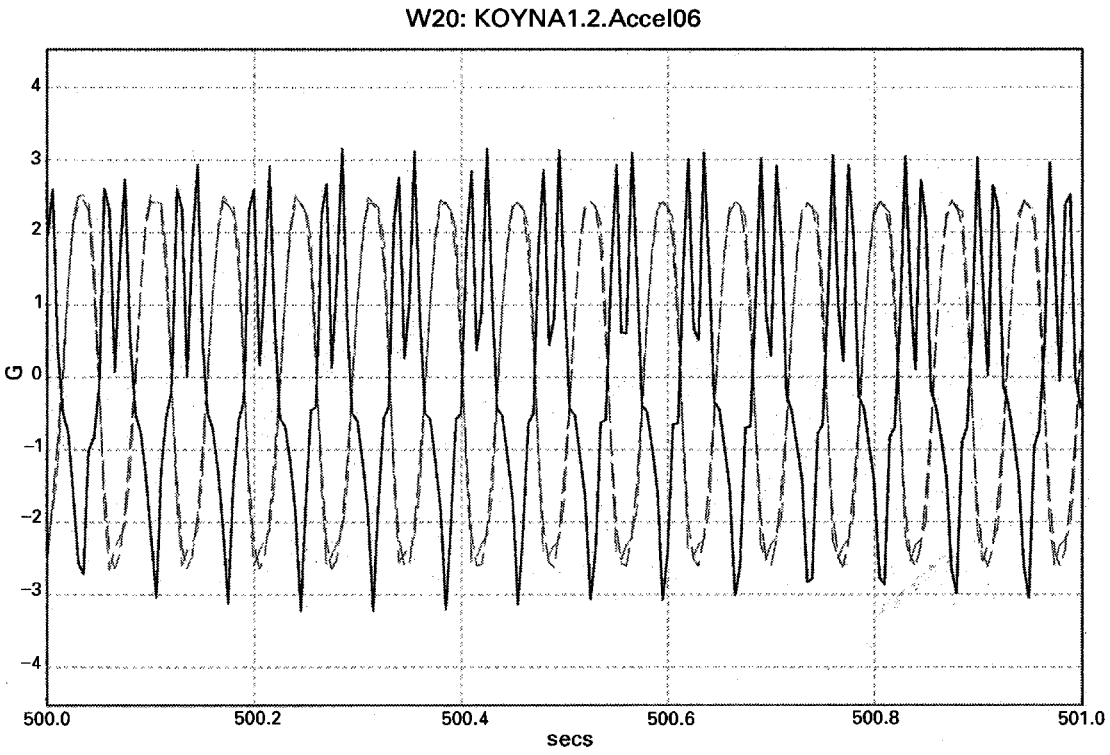

Figure 12. First Koyna model: base acceleration of 2.5*g*.

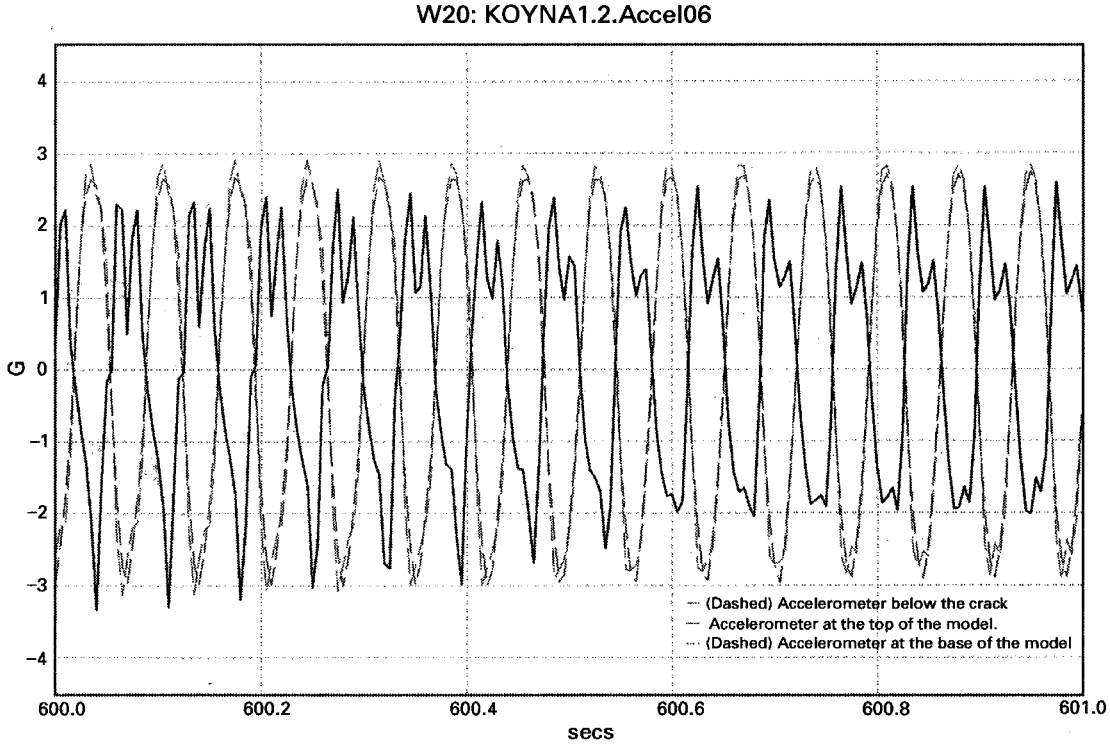

Figure 13. First Koyna model: base acceleration of 2.75*g*.

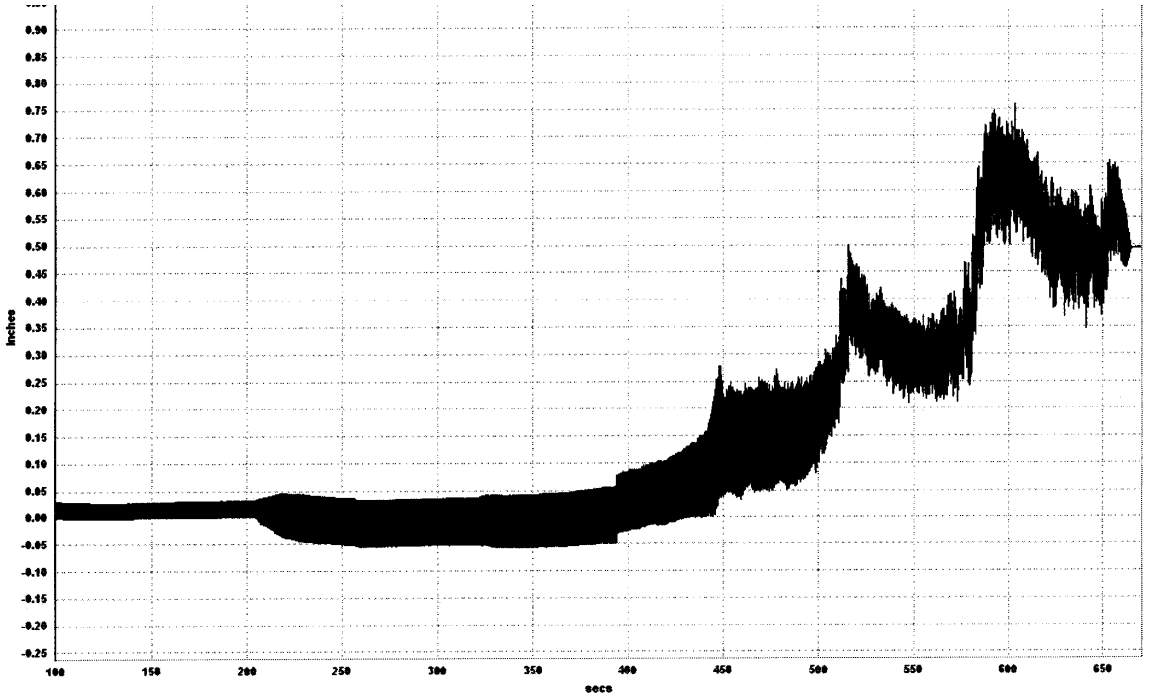

Figure 14 – First Koyna Model: Displacement at the top of the model.

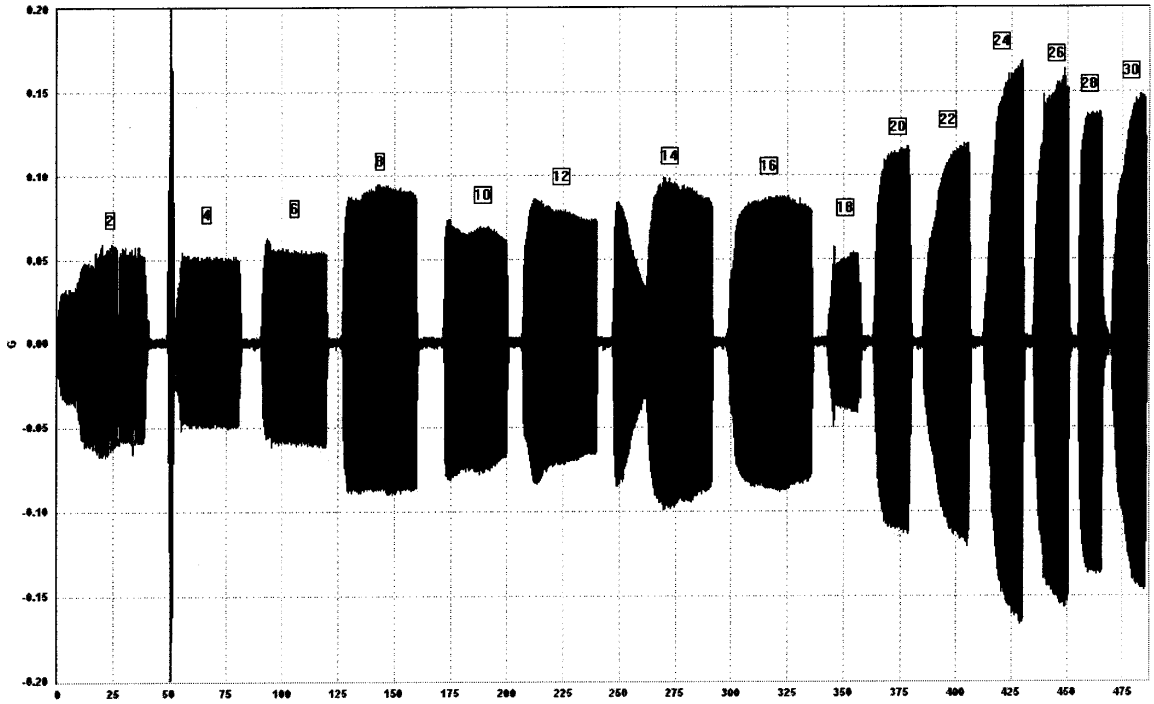

Figure 15 – Second Koyna Model: Frequency sweeps.

Finally, at a base acceleration of 2.75 g, the bottom motion is at a higher acceleration than the top of the dam (figure 13). By this time, the displacement of the top piece (approximately one-half inch) is well underway (figure 14), and the base motion is not readily transferred to the top section. The cross section maintained stability, and sliding progressed slowly during the input. The top block could be observed to be progressively sliding down the preexisting shrinkage crack surface.

Model 2—Monolithic Model

As with the first model, a modal sweep was completed first. Accelerations, normalized to the base motion and recorded during the sweep, are shown in figure 15. In comparing the modal responses with those for the first model (shown in figure 7), some differences are noticed in the response frequencies. In Model 1, 24 Hz seemed to indicate the first cantilever mode; whereas in model 2, this mode appears to emerge at 22 Hz. In both models, another increased response with respect to the input motion occurs at 28 Hz. These differences are believed to be inherent differences in the two models as built, but, generally, the two models appear similar in their modal response.

Model 2 was tested using the same strategy as the first model; that is, a 14-Hz sinusoidal motion was used and ramped in acceleration until failure. The total test duration using this method was almost 8 minutes. The final failure occurred at the change in slope of the model on a flat downward plane sloping toward the upstream face. The angle of the failure plane was 53 degrees from horizontal, which was 90 degrees from the lower slope in the bottom of the model, beginning at the invert. This angle is consistent with previous studies,[11] but was a single flat surface.

The model was videotaped during testing. Review of the tape revealed that the crack was not visible in one frame and had propagated completely by the next video frame. The standard video frame rate is approximately 1/30 of a second. With the input motion of 14 Hz, the period for one-half cycle would be 1/28 of a second. This indicates that the crack developed and propagated in less than 0.03 seconds, either during a stroke, or, more probably, at the reversal of a stroke. The base acceleration at the time of failure was 2.2 g.

Analysis of the test data revealed anomalous behavior beginning approximately 330 seconds into the test (figures 16-19). This behavior is best displayed in figure 18, which is the vertical acceleration of the model measured at the top of the structure. It can be seen that up to the 330-second point in the test, the vertical acceleration increases linearly with increasing horizontal input acceleration. This response is as expected and is attributed to a slight flexing of the shake table frame. At around 330 seconds, the vertical acceleration starts increasing dramatically and continues to increase throughout the duration of the test. This increase is accompanied by a corresponding decrease in the horizontal acceleration of the top of the structure, as seen in figure 17. The displacement of the top of the model is shown in figure 19, where a rather abrupt decrease in the displacement of the top appears. This change in

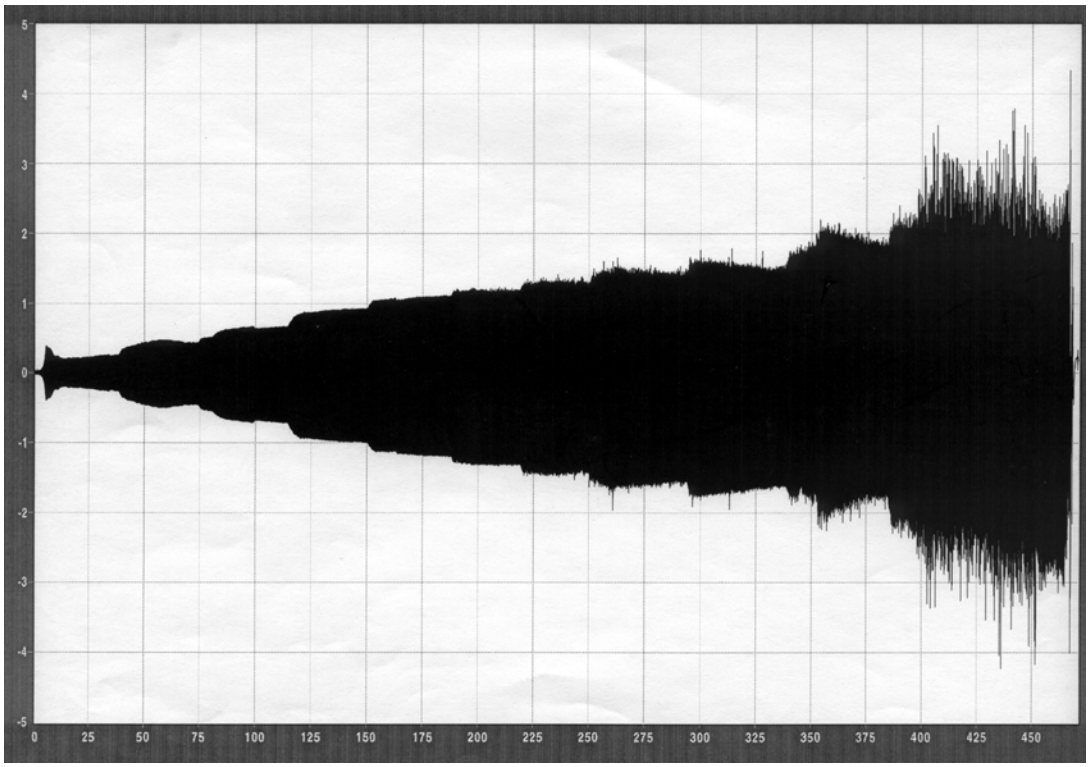

Figure 16.—Second Koyna model: horizontal acceleration at the base of the model.

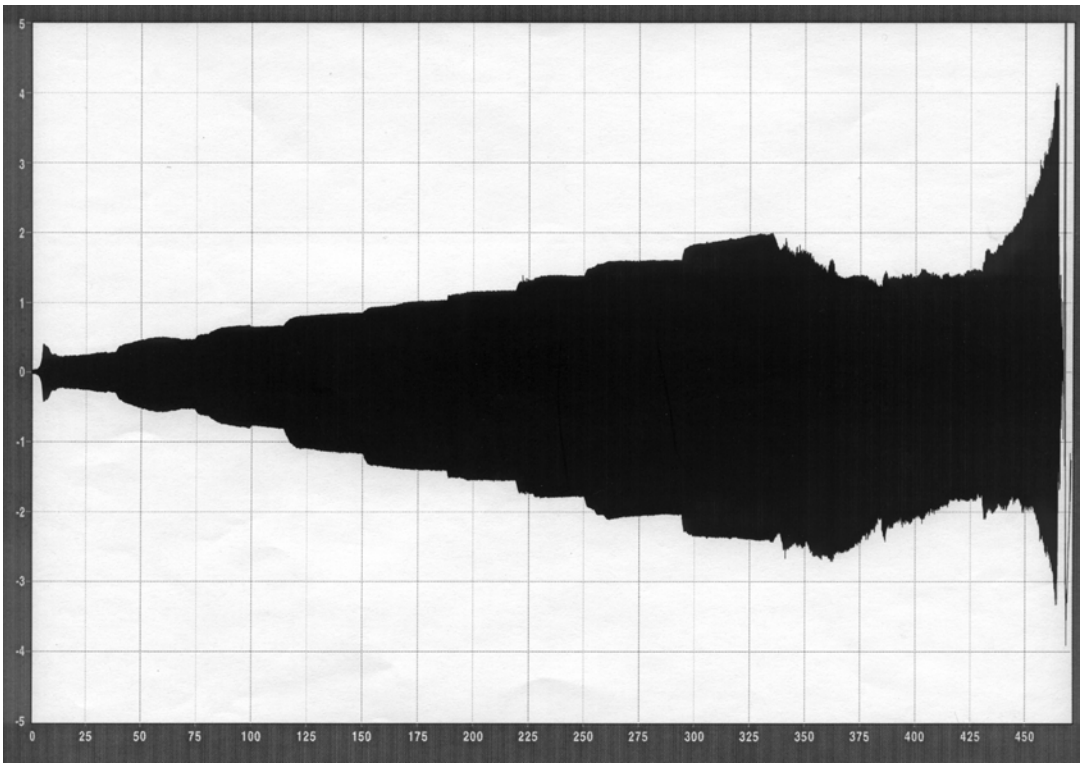

Figure 17.—Second Koyna model: horizontal acceleration at the top of the model.

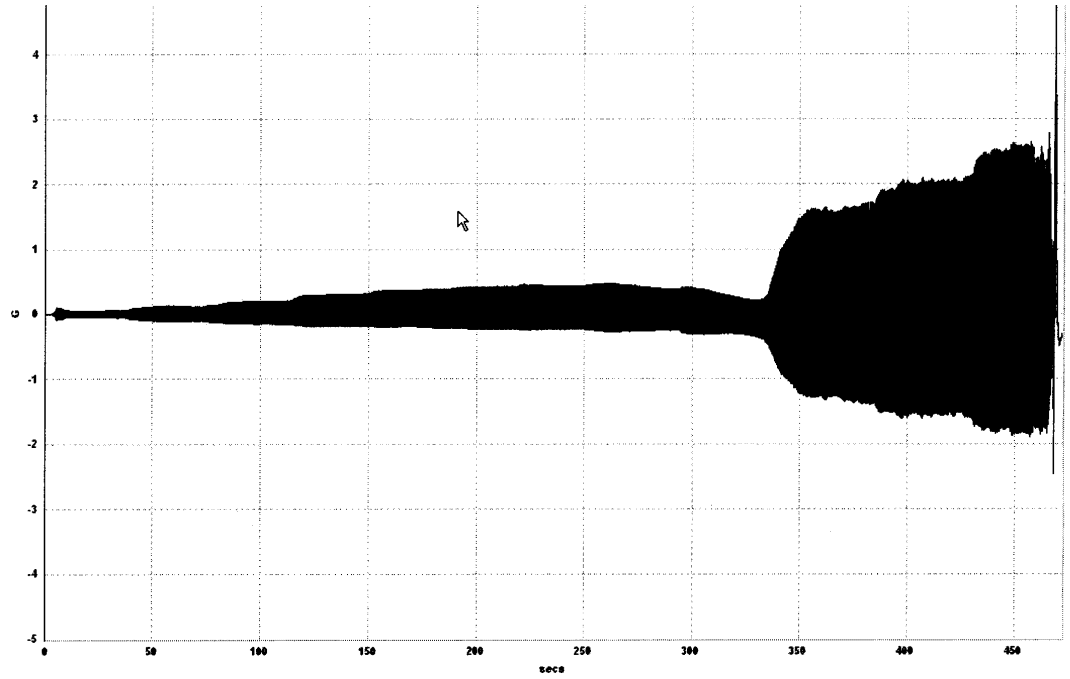

Figure 18 – Second Koyna Model: Vertical acceleration at the top of the model.

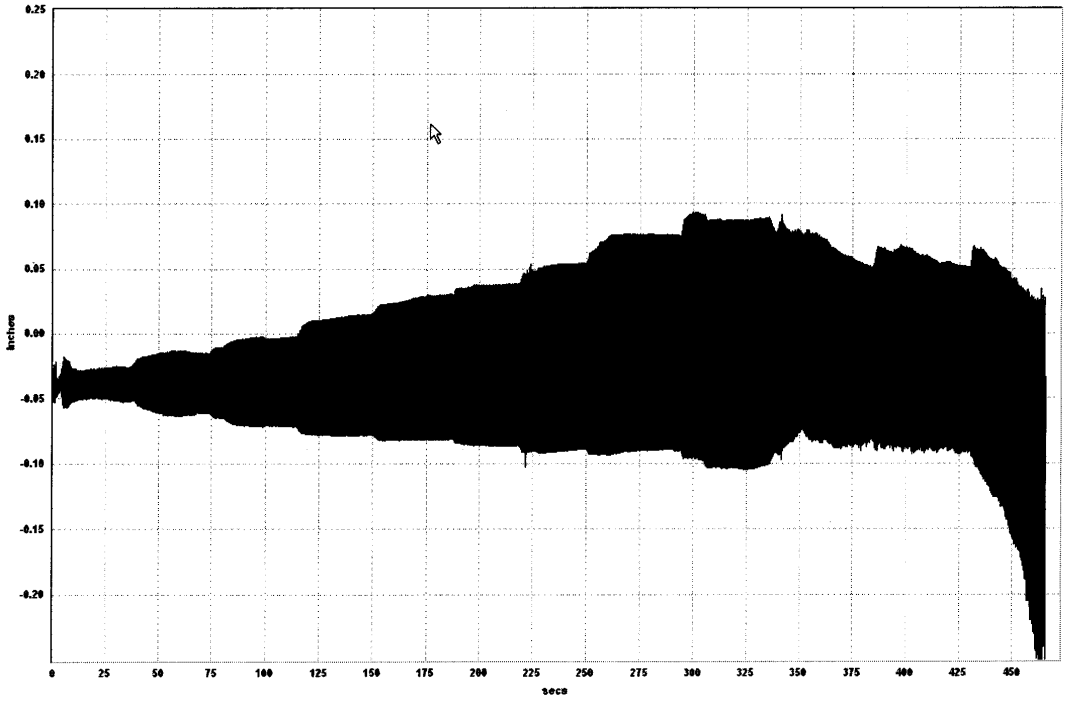

Figure 19 – Second Koyna Model: Displacement at the top of the model.

displacement would correspond with the decreased acceleration. These phenomena are not believed to be related to the failure of the dam portion of the model, but rather appear to be a failure in the base of the model which acted as the foundation of the structure.

The conclusion from these data is that the material around the all-thread embedded in the base started failing at around the 330 second time frame and allowed the model to rock. As more material failed, the rocking increased, which initially resulted in increased vertical accelerations and decreased acceleration of the top. Eventually, the material failure around the all-thread was severe enough that the entire model could slide back and forth a small amount in the direction of the excitation. This is evidenced by the spikes in base acceleration shown starting around the 400 second time frame in figure 16. This indeterminate boundary condition would be nearly impossible to model on a nonlinear analysis time-step basis. It is believed that general comparisons can still be made based on the final acceleration and the material properties presented.

It was noted that after initiation of the crack, the top of the model began to slide before toppling occurred. The top portion toppled from the model approximately 1 second (14 cycles) after crack propagation.

Conclusions and Discussion

1. A new low-strength concrete mix is proposed. This new concrete shows promise for use in similitude testing. The mix, which uses bentonite as the media to reduce strength properties, is readily adjusted to various scales with varying amounts of bentonite. The components may be mixed in mass and can be provided by commercial producers because no hazardous materials are used. Disposal is also easily accomplished by conventional methods.

2. The new mix produced strength and stiffness characteristics that nearly matched the similitude requirements. More importantly, for nonlinear modeling of the failure mechanism, the mix fails in a shear plane almost identical to conventional concrete.

3. The initially-cracked model and the monolithic model showed general mode shapes and damping which were similar for small accelerations.

4. The kinematically-nonlinear model (sliding model) demonstrated that there was some initial bond on a typical shrinkage crack, even on a crack visible to the eye on multiple faces, that needs to be overcome before sliding can be initiated.

5. Once sliding starts, the nonlinear effect creates very large changes in the dynamic response during a constant frequency sinusoidal input motion. The amplitude of the acceleration of the piece above the crack in this model actually becomes less than the amplitude of the acceleration of the base, and the response is phase shifted. Put simply, the base can slide back and forth beneath the top, and the motion is nearly uncoupled.

6. A material failure caused the monolithic model to fail. The material failure was characteristic of previous models and believed to be characteristic of cracks in the field.

7. During the monolithic test, a nonlinear change in the base fixed boundary condition created a highly nonlinear and indeterminate boundary condition. This nonlinear change also showed large changes in the dynamic response of the model. These changes are easily seen when compared to the constant input motion. Unfortunately, this same boundary condition change makes exact time history matching of numerical models impossible.

8. Both models failed at approximately 2.2 g of acceleration. In the kinematic model, the crack allowed a slow progressive sliding during the cyclic motion. In the materially nonlinear model, a crack was initiated in less than 1/30 of a second, and sliding occurred for a number of cycles before the top of the model toppled. The toppling is inconsistent with previous models and is believed to be related to the vertical accelerations caused by the boundary condition change.

9. Laboratory tests of the material were performed in conjunction with the shake table models to provide parameters typically needed in nonlinear numerical material models.

10. Results from the kinematic failure model (sliding) can conceivably be time step matched to verify nonlinear models. Results from the materially nonlinear models can be verified in a general manner to verify the cracking pattern and the acceleration required for failure.

Three-Dimensional Arch Dam Simulation

Background

Previous Work on Shake Tables

The arch section of the Techi Dam, Taiwan, has been modeled at a scale of 1/150.[3] A primary purpose of that study was to model the opening of joints; thus, the dam was articulated. The model was tested with motion in two planes: upstream-downstream and cross-canyon. Vibration mode frequencies were tested by suspending a weight from the model and subsequently cutting the weight loose to produce face vibrations. The El Centro Earthquake record was used in the shake table model test, with a time reduction of $\sqrt{1/150}$. Intensity was increased until the model collapsed. Significant joint degradation occurred at the arch end, probably because of local crushing at one end. In biaxial excitation, the arch collapsed with 1.34-g acceleration in the upstream/downstream direction and 0.91 g in the cross-canyon direction. The collapse occurred surprisingly close to the end of the excitation.

The same authors[12] noted that the test results showed significant nonlinear behavior. Significant influence of the joints generated increasingly poor correlations with the numerical analysis. Crushing in joints is suggested to improve analytical results.

Other tests have been conducted with shake table models[13] on smaller scale models at a scale of 1/100 and were tested to failure. A sinusoid input motion was used to determine characteristic frequencies of the structure. Next, similitude-corrected time histories of seismic events were used at increasing amplitudes to induce failure. Natural frequencies appear to be produced correctly when the modeled foundation is one to two times the height of the dam and extended laterally from the dam one to two times the height of the dam. The modeled length of the reservoir shows no significant effect with reservoir length being twice the dam height.

Test models have been completed to model sliding only.[14] Typically, these models were 1,000 mm in height. A short reservoir tank with absorbent rubber was used to eliminate the hydrodynamic effect (the length of the tank was 0.4 m). The following input motions used were: (a) a 7.5-Hz. sine wave (this waveform was hard to match exactly because some free vibration was present in the table); (b) 5 Hz ramped up in 5 cycles, held for 10 cycles, then ramped down in 5 cycles; and (c) a simulated earthquake of 12-second duration with the input ramped until slipping occurred.

Several models have been constructed to simulate failures in dams. One such model[15] was the Futatsuno Arch Dam. This 76-m-high, 210-m crest dam was modeled at 1/50 scale. In this model, the first crack *appeared* at 0.27 g and 32 Hz in a spillway pier, and at 0.41 g and 30 Hz on the dam. Final collapse occurred at 0.69 g and 17 Hz. The final failures are shown in figure 20.

Testing of models run to failure has been conducted at the ISMES facility in Italy.[16,17] The results are shown in figures 21 and 22 for wide and narrow canyons, respectively.

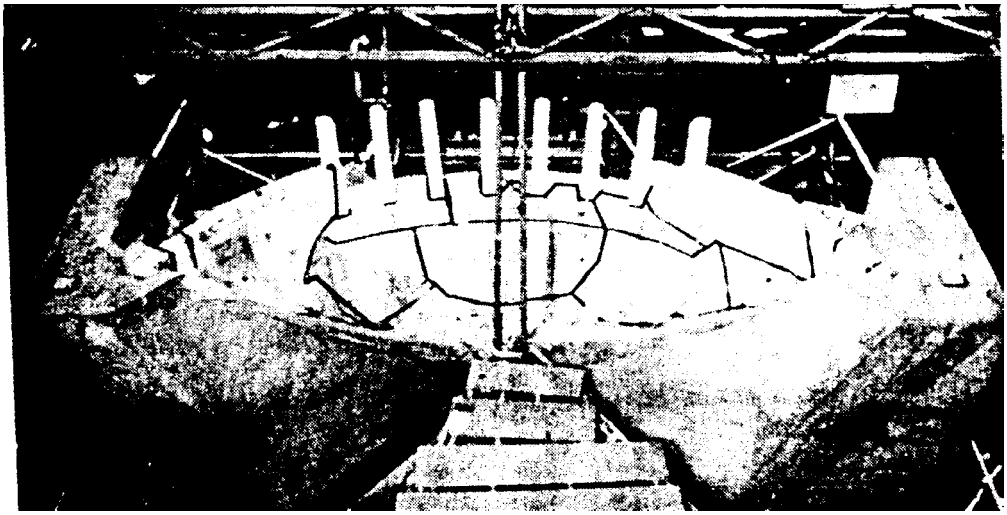

Figure 20.—Final failure of Futatsuno Arch Dam model.

Source: T. Yoshida and K. Baba, "Dynamic Response of Dams," Proceedings of the 3rd World Conference in Earthquake Engineering, Auckland, Vol. 2, 1965.

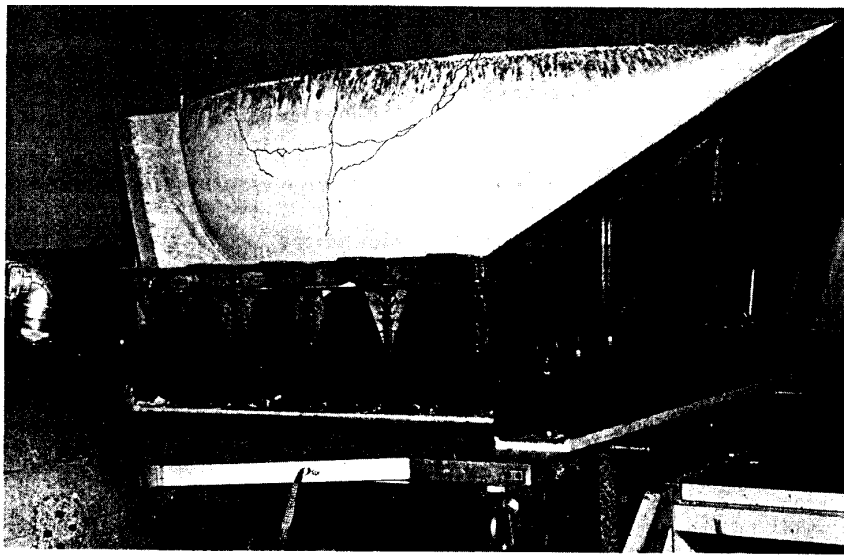

Figure 21.—ISMES wide arch dam model failure. Homogeneous dam shaken to failure with earthquake simulation.

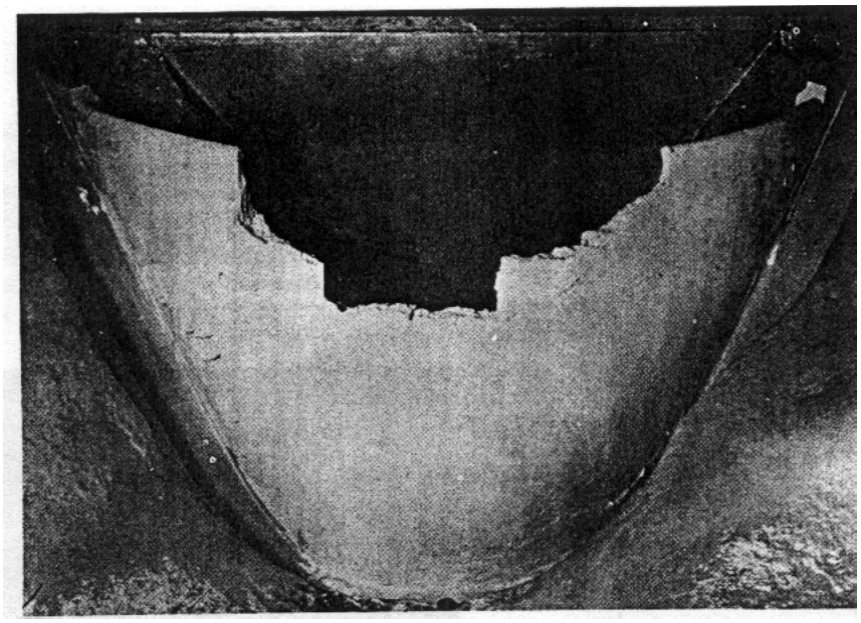

Figure 22.—ISMES test of narrow canyon dam model.

Source :

Oberti, G., and A. Castoldi, “The Use of Models in Assessing the Behavior of Concrete Dams,” Dams and Earthquake: Proceedings of a Conference held at the Institution of Civil Engineers, London, October 1-2, 1980.

Oberti, G., and E. Lauletta, “Structural Models for the Study of Dam Earthquake Resistance,” Ninth International Congress on Large Dams, Istanbul, Turkey, September 4-8, 1967.

Introduction

All the models chosen for this study were based on a similar geometry. Models were run in a sequence of: (1) a monolithic dam; (2) 1 horizontal joint at approximately mid-height; (3) 1 vertical joint at the mid-point of the valley; and (4) 17 vertical joints and 2 horizontal joints (one model was run with 17 vertical joints as a test of the construction method). All models were run with a sinusoidal input motion at 14 Hz, beginning at 0.25 g and increasing every 30 seconds by 0.25 g until a structural collapse was created in the model.

Experiment Setup and Procedure

The scale chosen for this model was a 1/150 scale. Similitude requirements for models have been summarized in other references.[8] Properties of mass concrete in dams have previously been published[18] and are summarized in table 5. For this study, typical values of properties were chosen as target parameters for the model and are summarized in table 6.

Table 5.—Averaged values of tested properties from dam core

Dam	Dynamic compressive strength (lb/in^2)	Dynamic modulus of elasticity (Mlb/in^2)	Dynamic tensile strength (lb/in^2)
Pine Flat	5,280	3.43	Unknown
Deadwood	5,930	3.83	690
Stewart Mountain	5,350	3.99	515
Roosevelt (saturated 1a)	4,090	4.21	755
Roosevelt (air dried 1b)	4,600	4.09	485
Roosevelt (saturated all other)	6,430	4.84	840
Roosevelt (air dried all other)	4,850	4.10	840
Roosevelt (12-inch diameter air cured)	3,730	5.70	575
Hoover	8,040	4.33	975
Folsom	4,760	4.50	510
Monticello	4,870	6.12	505
Englebright	6,660	4.63	585

Table 6.—Estimated concrete properties, the associated scale factors, and the model material target values

Property	Prototype estimate	Scale factor	Target value
E	5,200,000 lb/in^2 36,322,000 kN/m^2	150	35,000 lb/in^2 244,475 kN/m^2
f_c'	4,500 lb/in^2 31,432 kN/m^2	150	30 lb/in^2 209 kN/m^2
f_t	450 lb/in^2 3,143 kN/m^2	150	3 lb/in^2 21 kN/m^2
Density	150 lb/ft^3 2,403 kg/m^3	1	150 lb/ft^3 2,403 kg/m^3
ε_u^c	0.001	1	0.001
ε_u^t	0.0001	1	0.0001

Concrete Mix Design and Material Properties

In this study, a new, low-strength concrete mix was designed. Considerable work in this area has been accomplished in previous studies[2,3,9] to produce a similitude-appropriate concrete mix. Work from reference 19 was used previously with two-dimensional model studies in this laboratory. The advantages of this design were discussed previously. This design was modified for the 1/150 scale models of this study; the mix components and proportions are shown in table 7.

Table 7.—Model concrete mix components

Component	Lab mix (lb/yd^3)	Volume in mix
Air		0.14 (1/2% entrapped air assumed)
Water	739.8	11.86
Cement	156.6	0.8
Bentonite	63	0.39
Sand	2,245.41	13.81

Note: water/cement = 4.72 Bentonite/(Bentonite + Cement) = 28.7%

Early tests with this material demonstrated that all scaled parameters desired could not be met simultaneously. Specifically, the modulus of the material was on the order of 3,500 lb/in^2, and density was 118 lb/ft^3. With these constants, coefficients for calculating the required similitude relations were derived following the modeling theory developed in reference 24. The

coefficients used were: C_E = 4,500,000/3,500; C_ρ = 150/118; C_s = 150, where C_E represents the coefficient for modulus, C_ρ represents the coefficient for density, and C_s is the scale factor. Table 8 introduces the strength and stiffness and the series of models produced for this study.

Model Construction and Instrumentation

The tests were performed in the U.S. Bureau of Reclamation, Materials Engineering and Research Laboratory. The Vibration Laboratory is used for large-scale tests and has been in existence at Reclamation since 1969[10]. For these experiments, a shake table was constructed that has movement constrained to a single axis (horizontal only). The table was tested for its response modes and also tested in motion with accelerometers to determine its capabilities for use at higher frequencies. The table responded well for input frequencies below 22 Hz, which was below the table's lowest natural frequency of 30 Hz, but higher frequencies were eliminated for testing. Response of the table was clearly best at frequencies of 26 Hz and below. For this reason, a similitude simulation of an earthquake motion was not used. Rather, for practical reasons associated with the table, and for simplicity in numerical model calibration, a sinusoidal motion was selected.

The selection of the frequency of the motion was based on the similitude coefficients and typical values of natural frequencies of dams tested onsite. The frequency conversion similitude coefficient becomes:

$$C_f = C_s \frac{\sqrt{C_\rho}}{\sqrt{C_E}}$$

For this model, the scale (C_s) is 1/150. Considering the range of modulus values of the materials in various models (C_E), a range of frequency coefficients would be from 4 to 5.36. Table 9 shows typical measured values of natural frequencies for specific dams. A typical 1st mode natural frequency of 3.3 Hz was chosen for a wide valley structure. Applying the range of similitude coefficients to this frequency yields a range of model scale frequencies from 12 to 16 Hz and, hence, the chosen excitation frequency of 14 Hz.

Results and Indications of the Models

In-Situ Tests for Modal Shape and Frequency

The model modes were physically tested using frequency sweeps at very low accelerations (0.5 g). The low acceleration was chosen to ensure that the model would not be damaged during the frequency sweeps. Unfortunately, the low excitations did not produce sufficient displacement for a conclusive determination of the model's dynamic properties.

Table 8.—Models with associated properties

Model	Type	Date	Age (days)	Average comp. (lb/in^2)	Average split (lb/in^2)	Average beam (lb/in^2)	E	Failure acceleration, g	
								Initial crack	Final failure
M-1	Monolith	3/12/99	7	28.1		3.2			
M-2	Monolith	3/31/99	7	23.25		4	2,303	.75	5.0
M-4	Monolith - 1st pulse	7/28/99	6	33.64			3,761		
M-5	Monolith	8/12/99	6	37.5	4.83	3.1	3,088.4		
M-6	Vertical joint (saloon door)	8/27/99	7	25.6	4.67			0.7	0.85
M-7	Vertical joint	5/2/00	8	40.3				1.5	1.5
M-8	Vertical joint	6/21/00	7	28.2				1.5	1.5
M-9	Horizontal joint	7/19/00	7	36				0.95	1.75
M-10	Horizontal joint	8/2/00	7	52.1			5,172.1	1.65	1.65
M-11	Vertical joint	8/22/00	6	41.97	4.4		3,758.8	1.2	1.2
M-12	17 vertical joints	10/3/00	5	27.01			2,146.6	0.6	0.6
M-13	17 vertical joints	4/10/01	5	23.2	3.58		3,461.47	0.5	0.5
M-14	2 horizontal, 17 vertical joints	4/24/01	5	19.625	3.09		3,099	1	1.25
M-15	2 horizontal, 17 vertical joints	5/1/01	5	21.4	4.05		3,947.9	0.75	0.75

Table 9.—Typical frequencies of dams[20,21,22,23,24]

Dam	Reservoir level	Frequency (Hz)					Damping (%)				
		Sym			Asym		Sym			Asym	
		1st	2nd	3rd	1st	2nd	1st	2nd	3rd	1st	2nd
Kamishiba	Full	3.8	5.8	8.7	4.3	7.2	5	4	4.5	4	4.5
	Low	-	6.3	9.7	4.7	8.0	-	4	4.5	4	4
Sazananigawa	Full	5.5	6.8	-	4.3	8.7	2	3.7	-	3	2
	Low	6.7	-	-	5.5	-	1.8	-	-	1.8	-
Monticello	-	3.13	4.68	7.60	3.55	6.00	2.7	2.5	2.4	2.2	2.1
Morrow Point	-	2.95	3.95	5.40	3.30	6.21	4.0	3.9	4.3	1.5	3.3
Alpe Gera Gravity	78%	3.25	-	-	4.56	-	5.4	-	-	5.12	-
	Empty	3.47	6.16	-	4.72	7.43	4.4	4.50	-	4.50	3.43
Fiastra Gravity	88%	4.72	7.87	-	5.97	9.72	3.27	2.38	-	2.46	2.50
	72%	4.29	7.34	-	2.56	9.16	3.30	2.80	-	7.34	2.50
Place Moulin Arch	95%	2.03	3.63	-	2.03	2.96	1.15	1.20	-	1.18	1.22
Talvacchi Arch	90%	3.8	5.35	-	3.68	6.7	3.5	3.5	-	3.5	3.5
Barcis Arch	Full	10.1	15.3	-	7.6	16.3	4	4	-	7.0	3.5
Ambiesta Arch	Full	4.27	7.3	-	3.90	-	3.02	6.65	-	2.15	-
	94%	4.7	-	-	2.0	-	1.9	-	-	4.7	-

Linear Versus Nonlinear Structural Behavior

The models all acted in a structurally linear manner until the onset of cracking. This was evidenced by a characteristic mode shape and increase of acceleration from the base of the dam to the top of the dam. This pattern is shown for the monolith, horizontal joint, vertical joint, and 17x2 joint models in figures 23 through 26, respectively. These figures all show time plots of acceleration over a fairly broad period. From the plots, the increase in acceleration of the top versus the base of the dam is shown in the overlay of data. The initiation of cracking causes a nonlinear effect, which results in a change in the pattern. A good example of this is shown in figure 24, with an obvious change in response. In figure 25, another model is shown with an expanded scale time. What is clear in all the figures is that there is a linear increase of acceleration with height until the initiation of cracking. When cracking occurs, this linear behavior changes rapidly. This sudden and extremely different nonlinear behavior is highly dependent on joint type, as described in the next section.

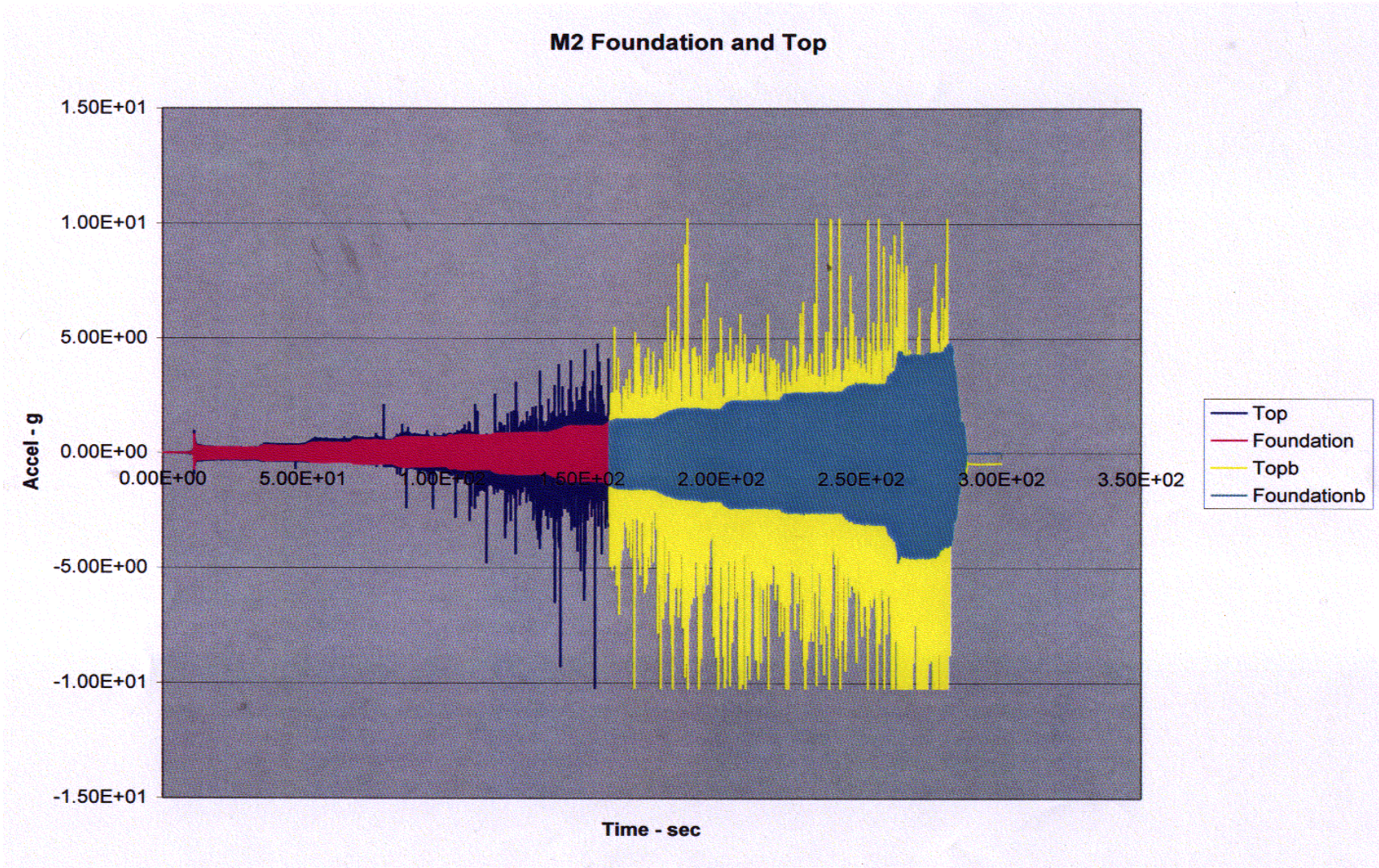

Figure 23.—Model 2 - monolithic model accelerations.

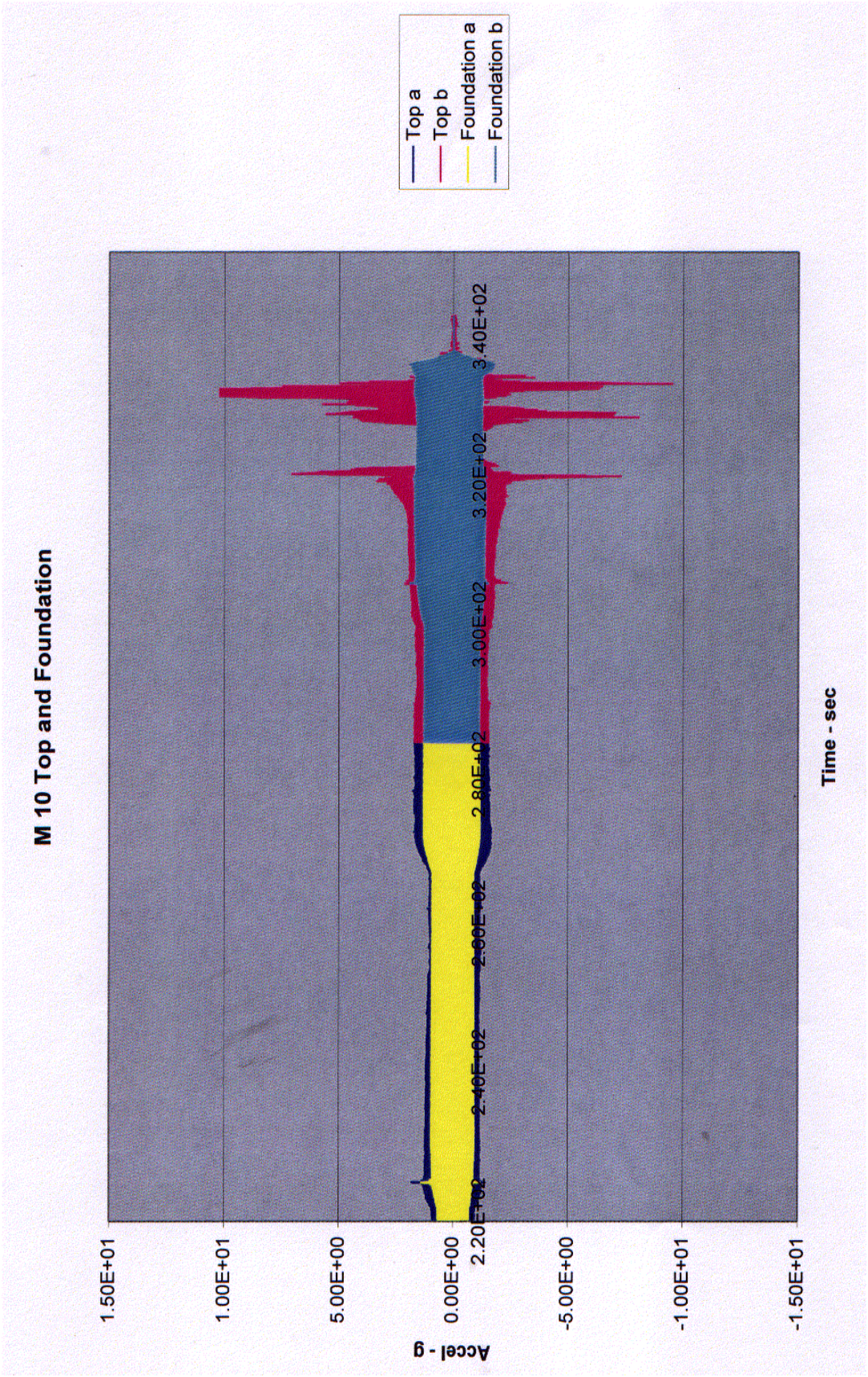

Figure 24.—Horizontal-joint model accelerations.

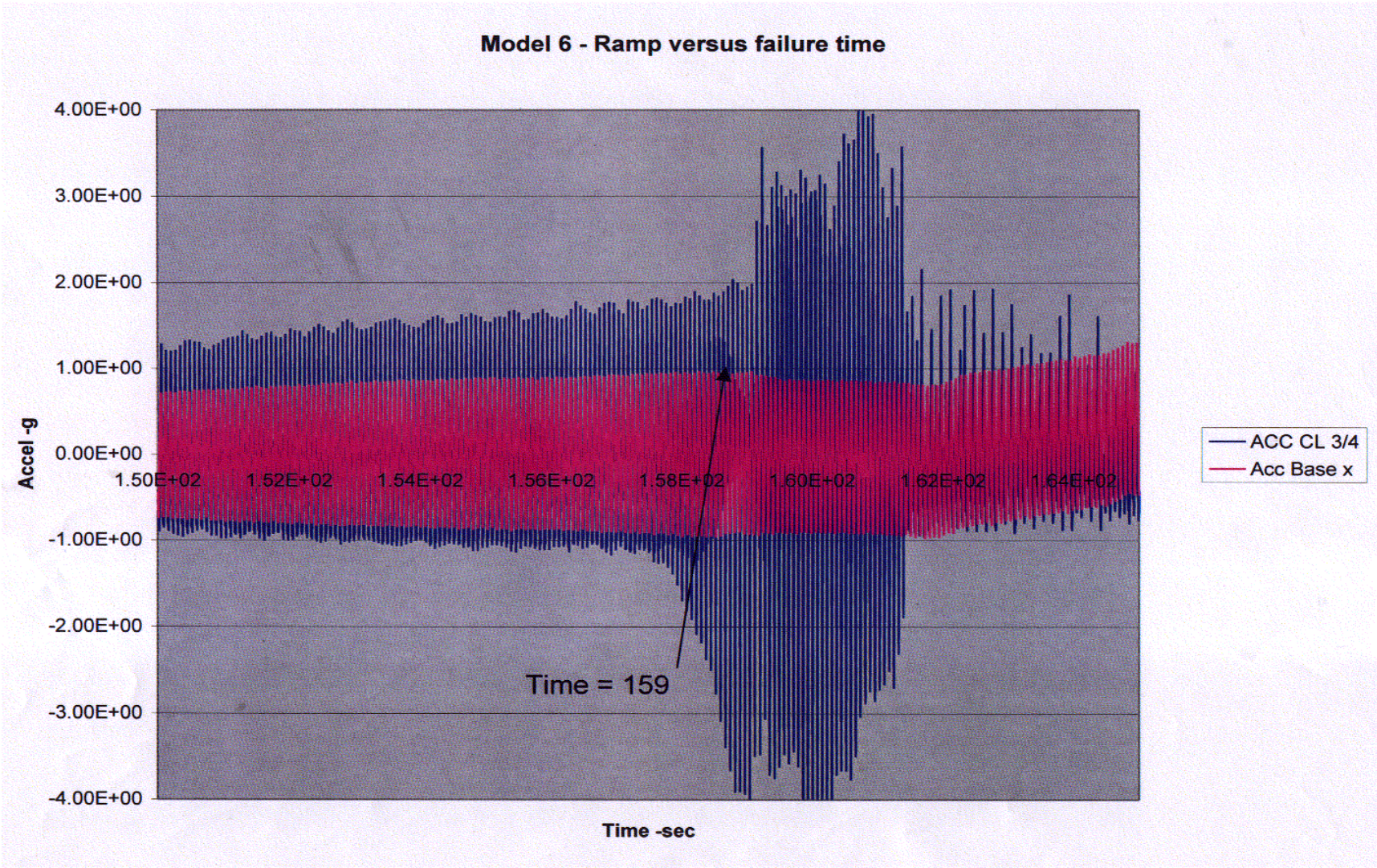

Figure 25.—Vertical-joint model accelerations.

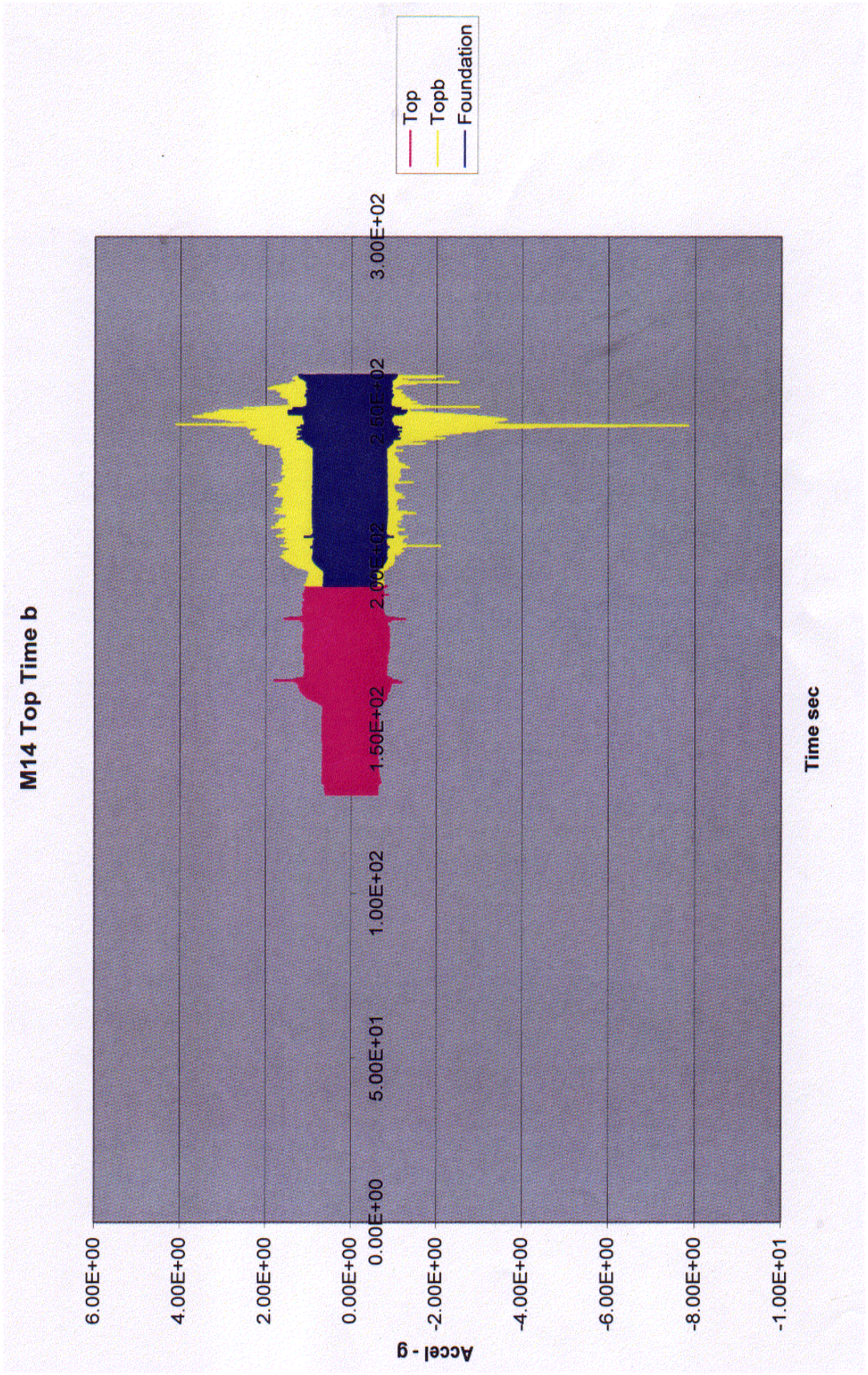

Figure 26.—17x2-joint model accelerations.

An investigation of the linear effect for different types of models is shown in figure 27. To study the initiation of cracking of all models uniformly, an estimate of the initial cracking acceleration was made through a normalization calculation. One stiffness value was chosen as a reference value, and all accelerations that caused initial cracking were normalized by using the ratio of the reference value to the modulus value within each model. This ratio was then used to adjust the acceleration within an individual model which caused initial cracking. This figure shows that, for this model, cracks generally occurred at an acceleration of 0.70 g. Because all models are linear until the initiation of cracking, this parameter is unaffected by model type.

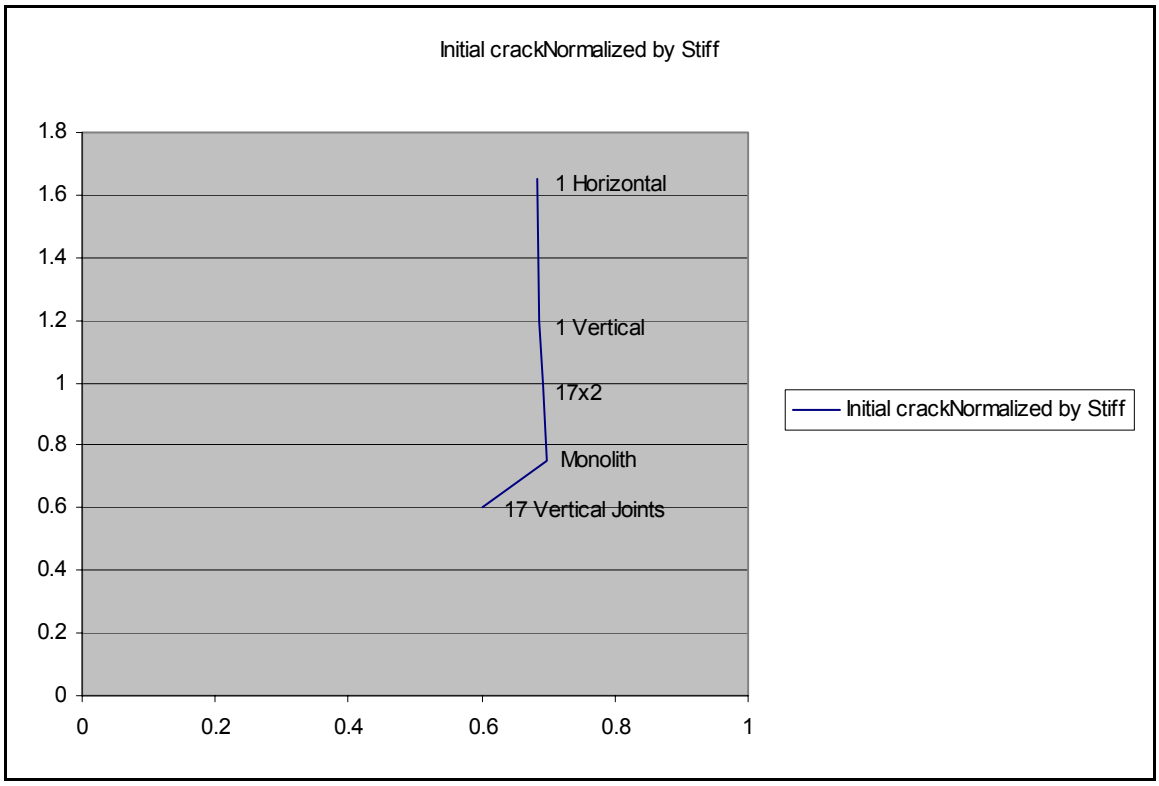

Figure 27.—Initial crack normalized to stiffness.

Effect of Joints on Nonlinear Behavior

Photos of the different models are shown in figures 28 through 31. These models employed the different jointing patterns of monolith, horizontal joint, vertical joint, and multiple joint, respectively. From these figures, it is easily seen that the joint patterns have a great effect on the initial and final cracking patterns. Figure 32 shows all initial cracking patterns overlaid on the same picture. The joints control the initial cracking pattern. The monolith breaks initially into one fairly large piece from approximately one-fourth of the distance across the canyon, down to about the one-fourth of the height, and then up the centerline. All other patterns are controlled by the joints. A deep crack occurred along the vertical joint, and the horizontal joint forms the predominant pattern in the first crack. In the 17x2 joint case, the upper horizontal joint forms the predominant pattern. There are three vertical joints in the initial pattern.

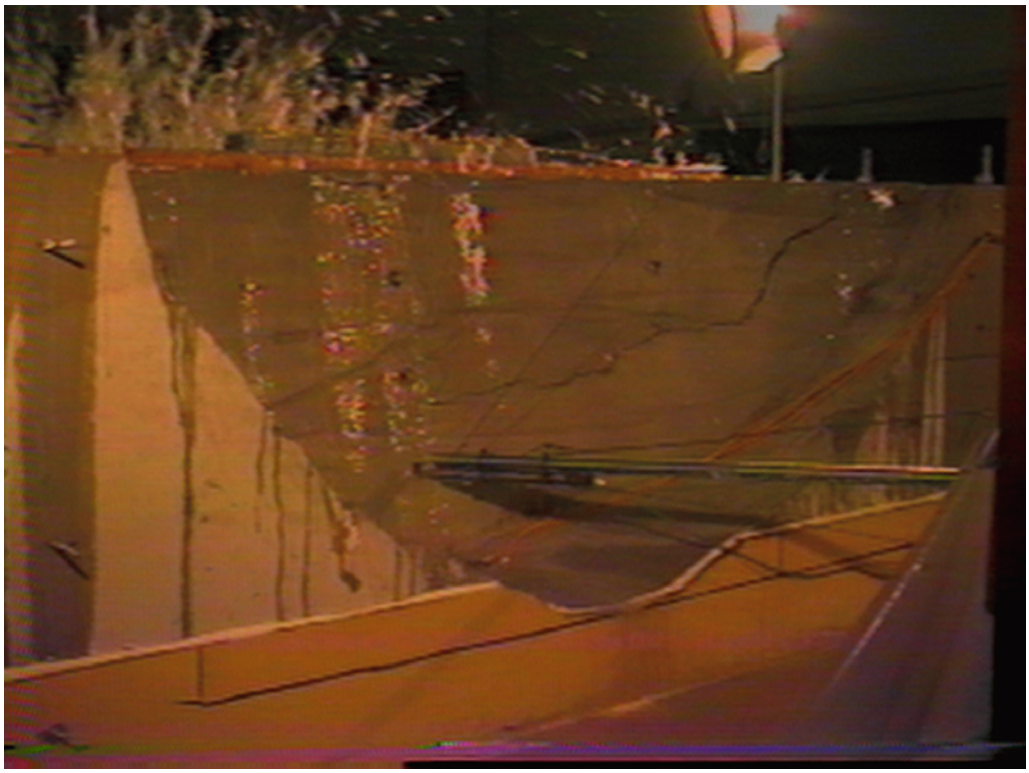

Figure 28a.— Monolithic model 2, initial cracking.

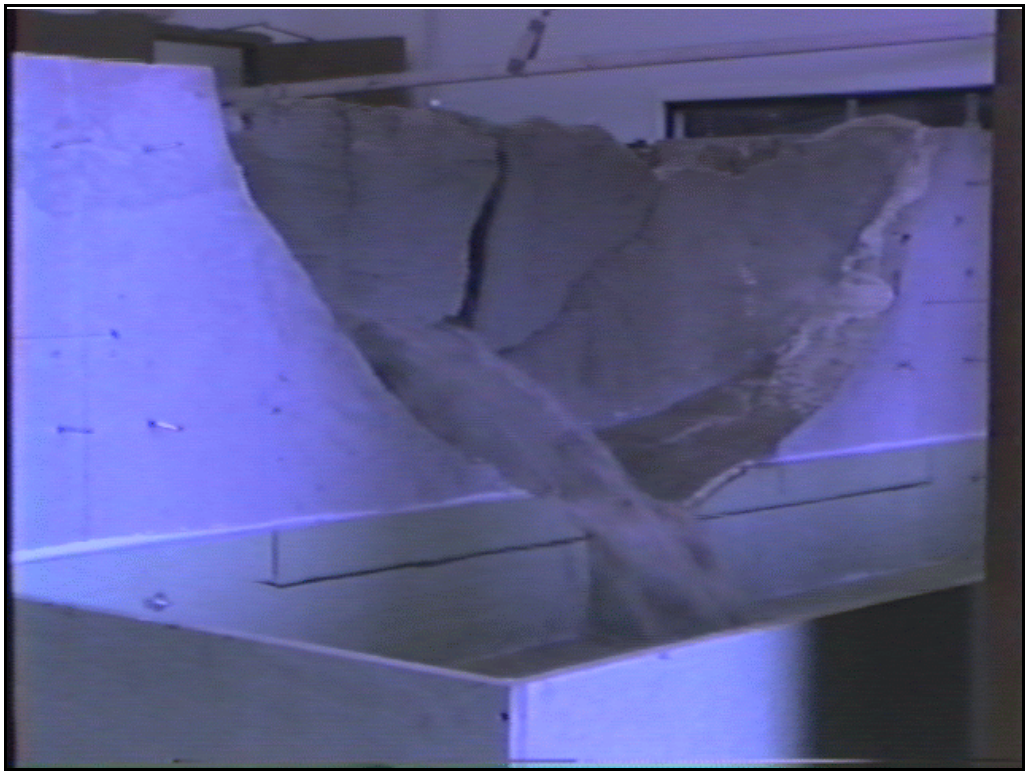

Figure 28b.—Monolithic model 2, final crack.

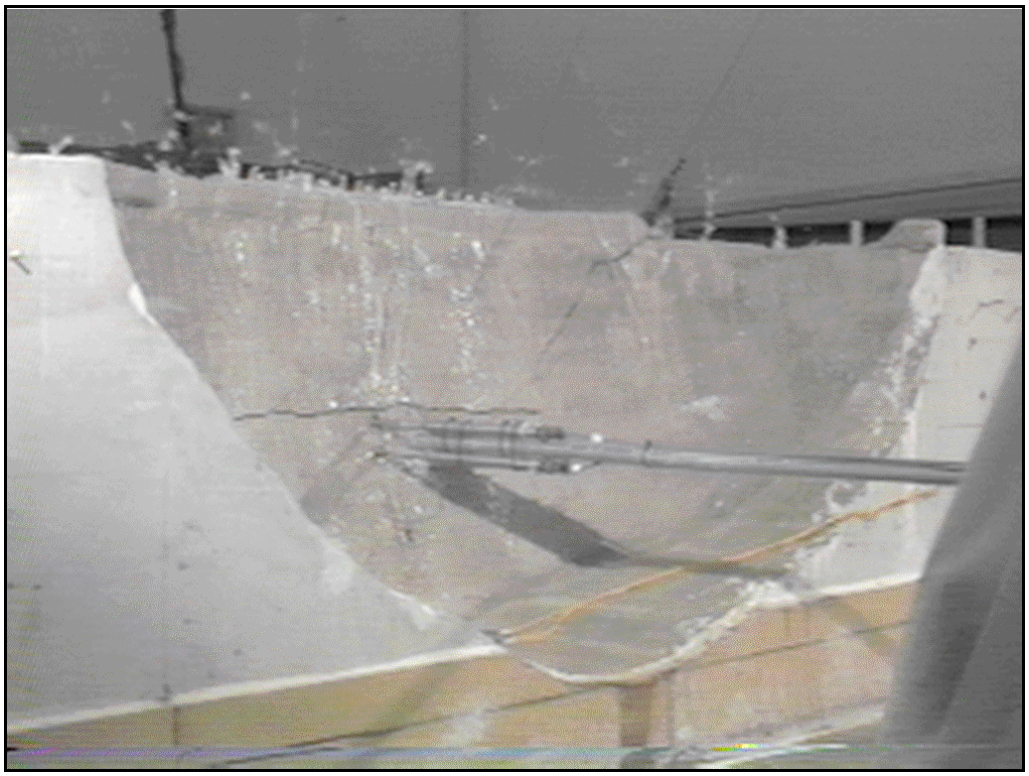

Figure 29a.—Model 10 - horizontal joint initial failure, south camera.

Figure 29b.—Model 10 - horizontal joint final failure.

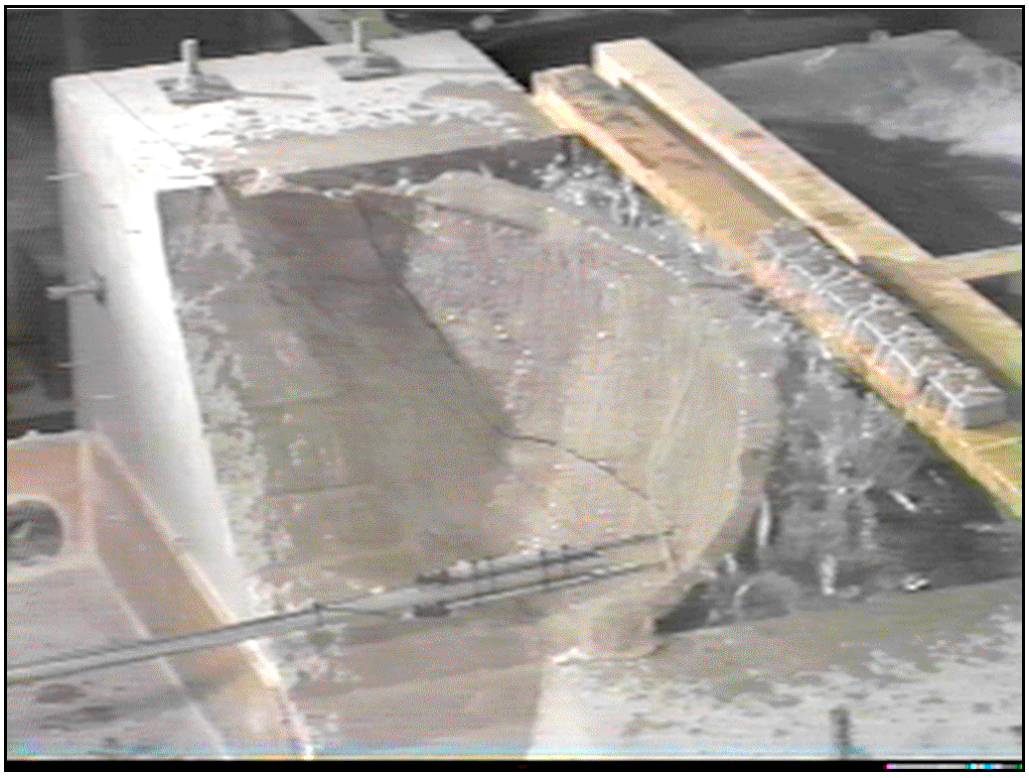

Figure 29c.—Model 10 - horizontal joint north view, initial cracking.

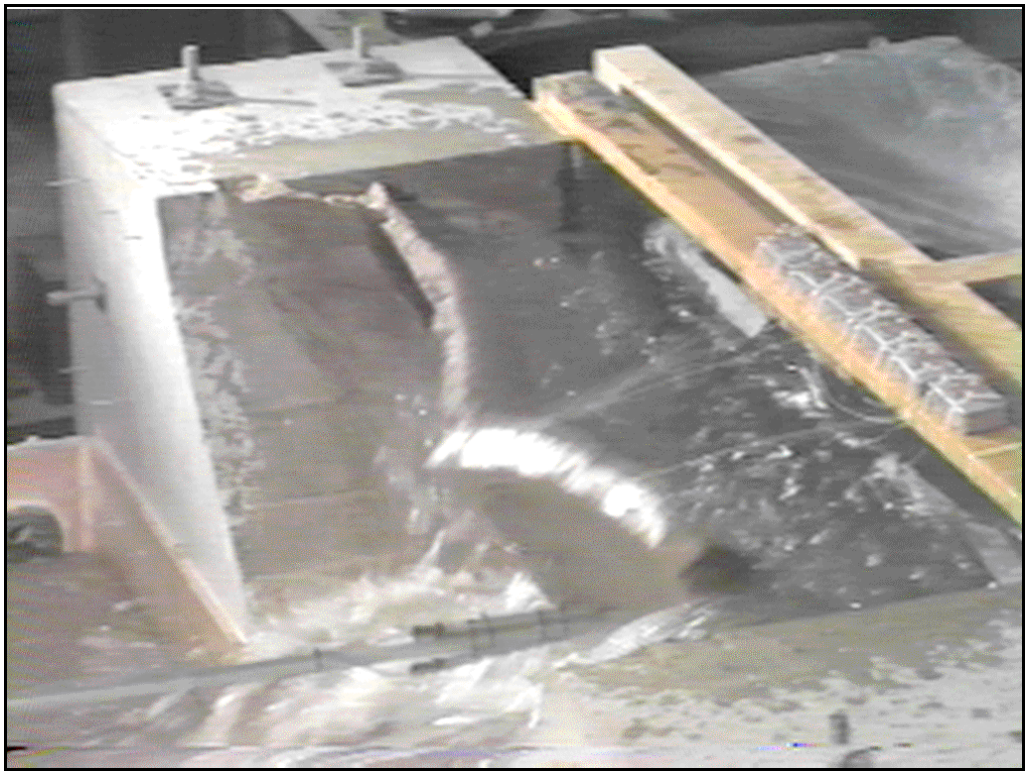

Figure 29d.—Model 10 - horizontal joint north view, final failure.

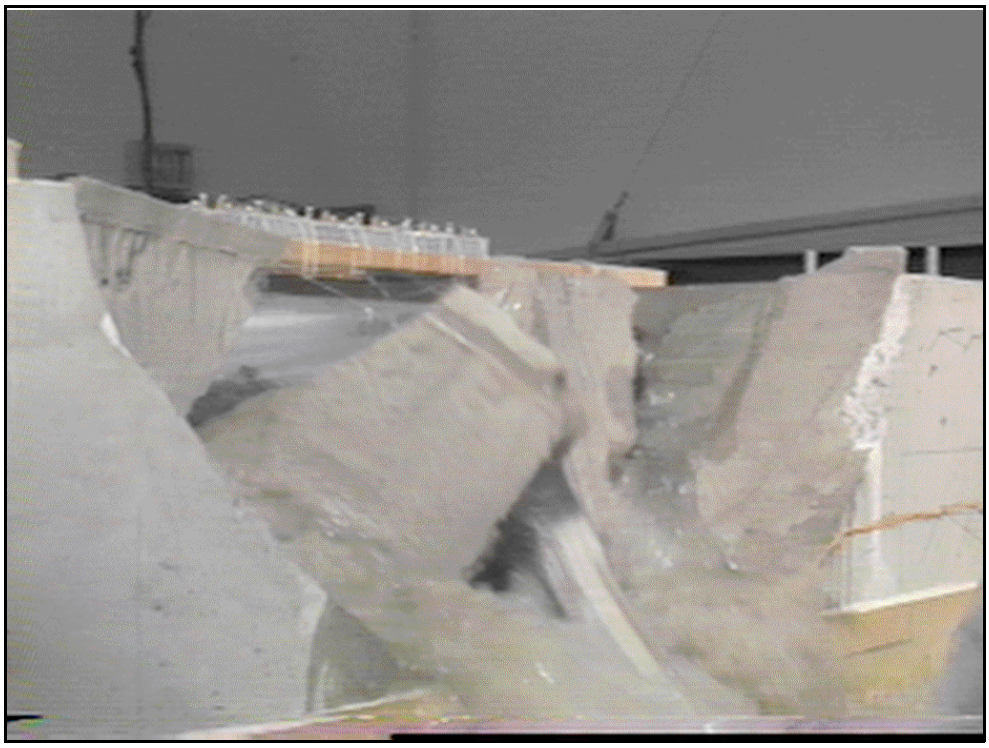

Figure 30a.—Model 11 - vertical joint south view, final failure.

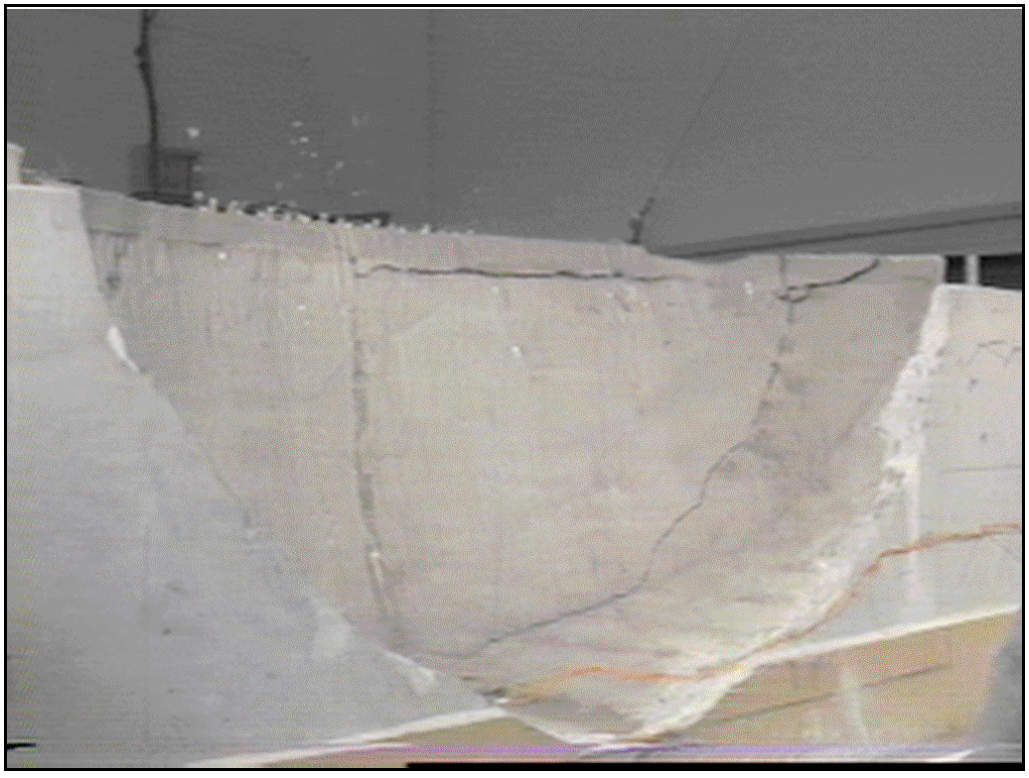

Figure 30b.—Model 11 - vertical joint south view, initial cracking.

Figure 30c.—Model 11 - vertical joint north view, final failure.

Figure 30d.—Model 11 - north view, initial cracking.

Figure 31a.—Model 15 - 17x2 joints, initial cracks.

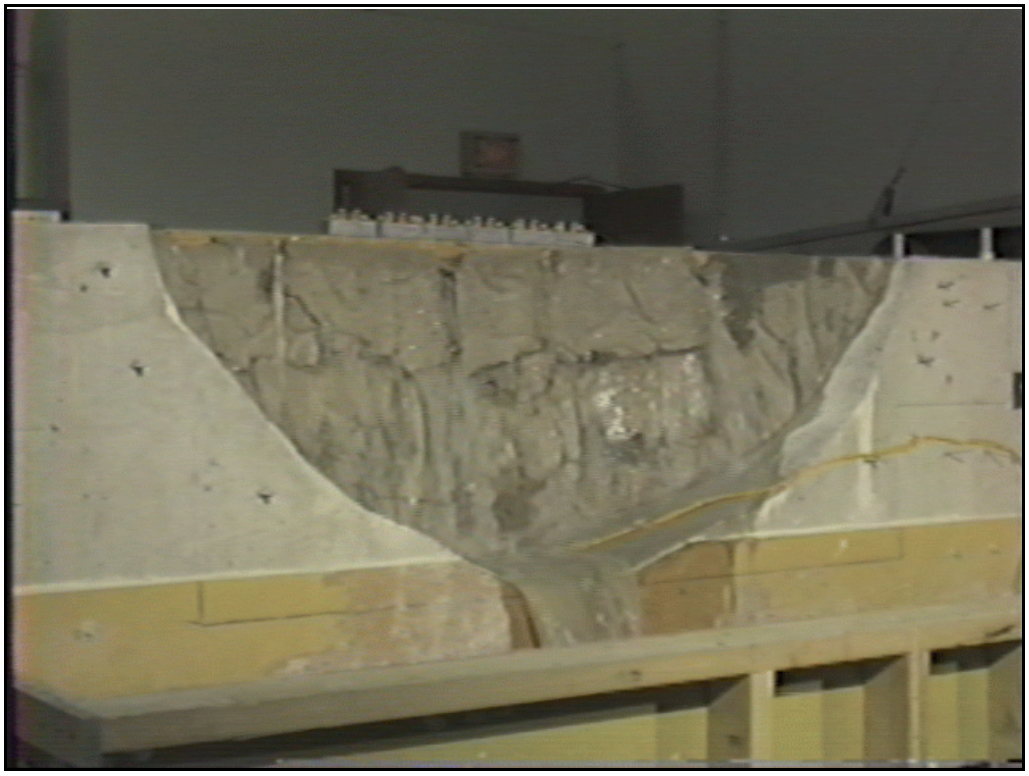

Figure 31b.—17x2 joints, final cracks.

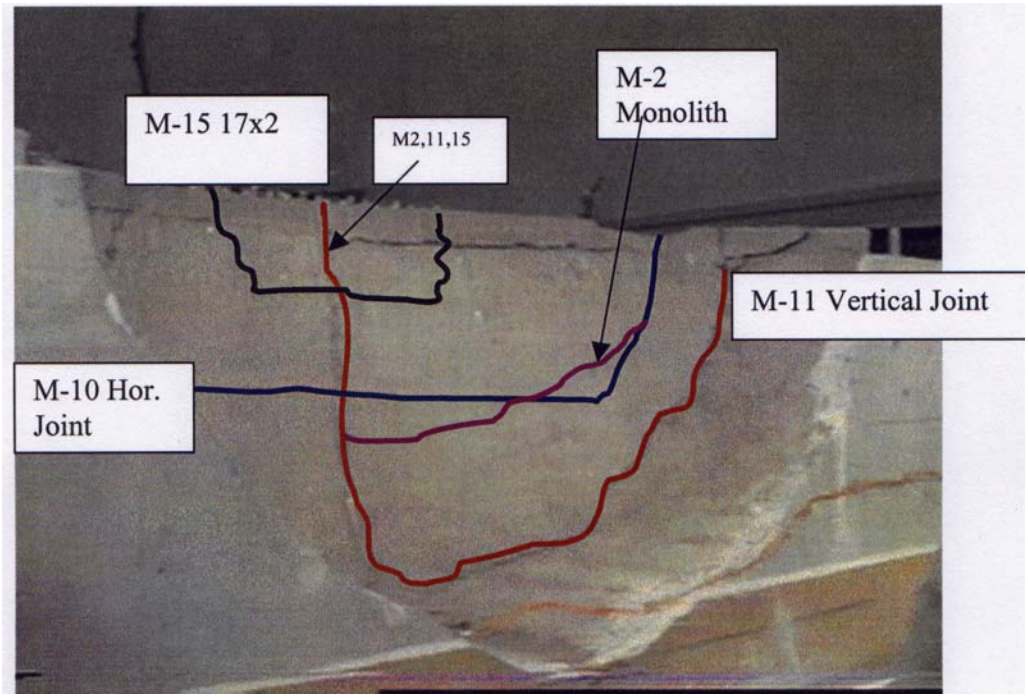

Figure 32.—Approximate location of all initial cracks in different models.

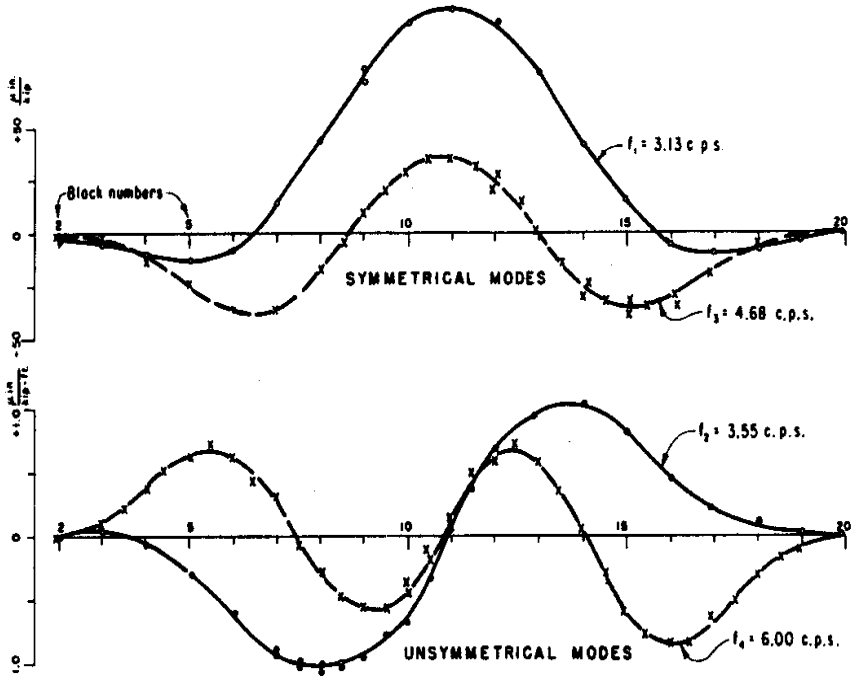

Figure 33.—Mode shapes for typical dam, measured in the field.[24]

The final crack pattern is different for each model, showing once again the influence of the constructed joints. Figure 34 shows the final pattern for the 17x2 model, with the mode shapes superimposed in a way that accounts for the rotation of the photograph from the on-face plane). The pattern of the formation of five large blocks in the failure mode is somewhat common in all models and might be suggested as a pattern that is consistent with the modes of the structure. The final failure in all models occurred after considerable time, following on the order of 20-30 seconds of shaking after the initial crack. This is consistent with comments by other authors[12] and is most likely associated with the need to abrade joints to provide sufficient space for the blocks to snap through in the downstream direction.

Effects of a Wide Canyon

Figure 35 shows the initiation of failure in the dam at the 1/4 point across the canyon and the centerline of the dam. The accelerations show that: (1) the onset of nonlinearity occurs first in the centerline and about one-half second later at the quarter point. Although this seems like a small difference, accounting for the time similitude of 12.8 times for the model to fail, this difference is 6.4 seconds later in real time, which is a significant portion of an earthquake record; and (2) degradation of the acceleration of the 1/4 point is almost immediate, whereas there is a time period of approximately 2 seconds of increased motion in the centerline before the degradation of acceleration is observed.

Water in Joints

One additional issue for consideration is the ability of water to penetrate joints during the earthquake. Figure 36 shows a crack forming and water being shot from this crack in three cycles of the test (1/10 of a second). It is noted that the fluid used is water, without adjustment for viscosity similitude. Nevertheless, water is clearly seen traveling through the dam in this sequence.

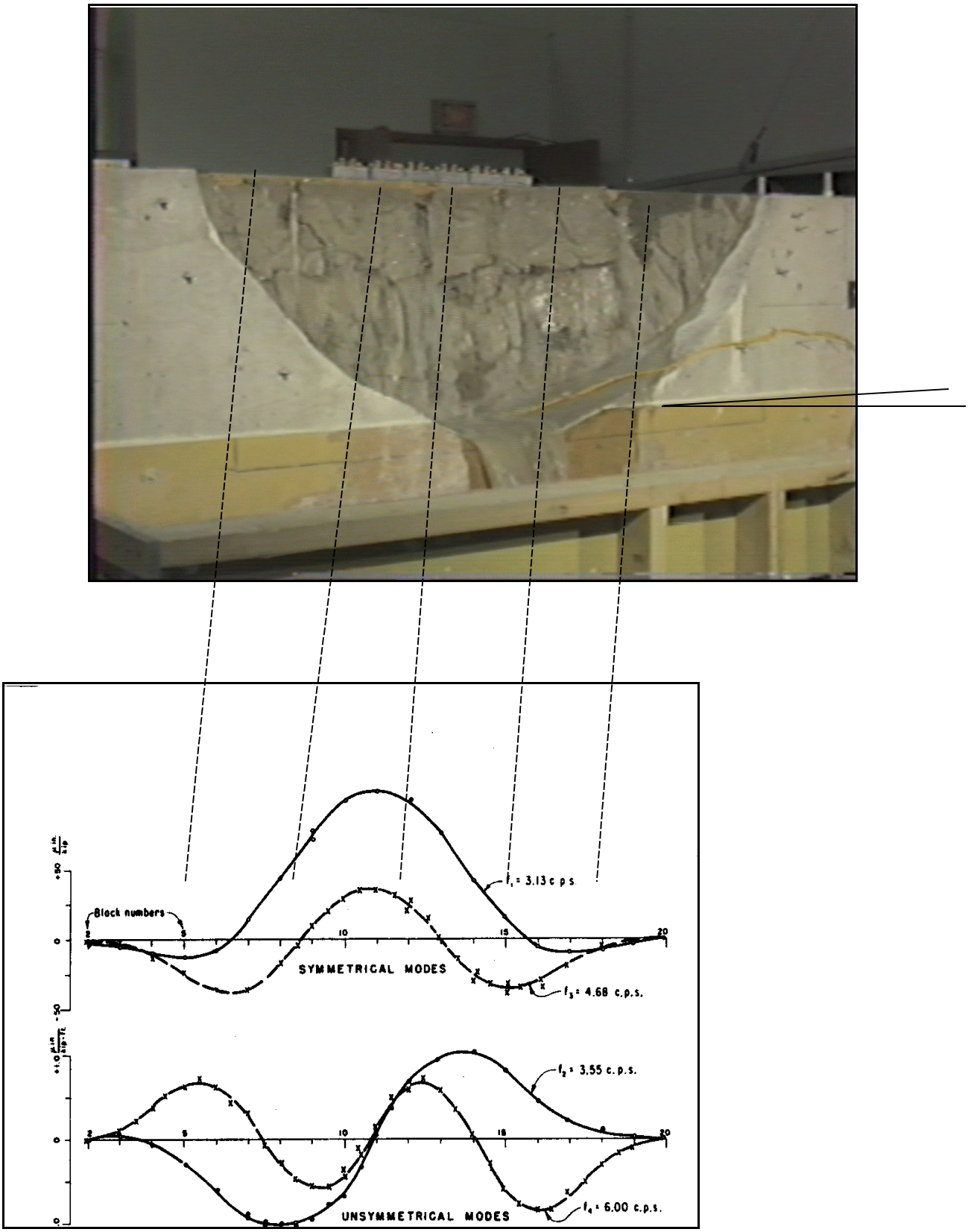

Figure 34.—Final crack pattern and mode shapes.

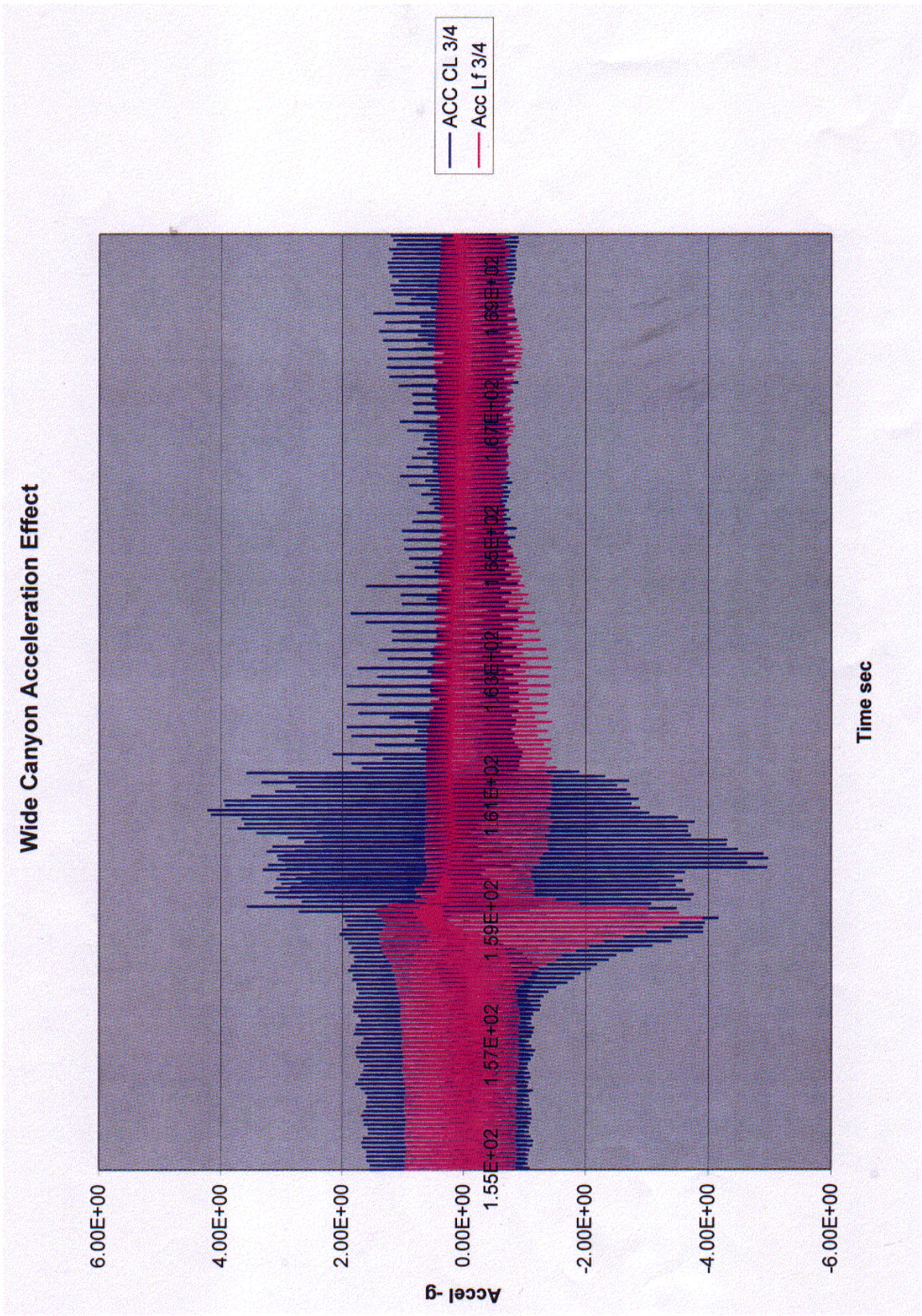

Figure 35.—Cracks accounting for wide canyon effects.

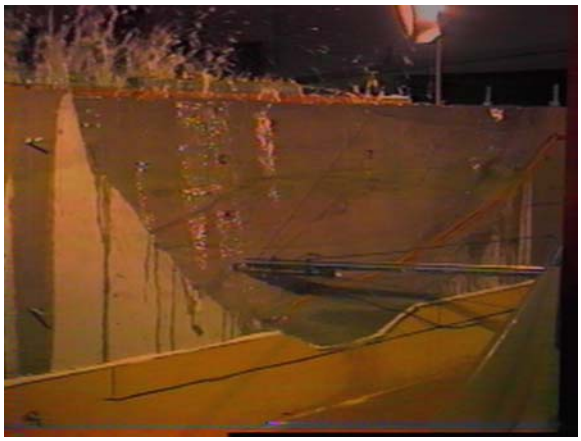

Crack Initiates

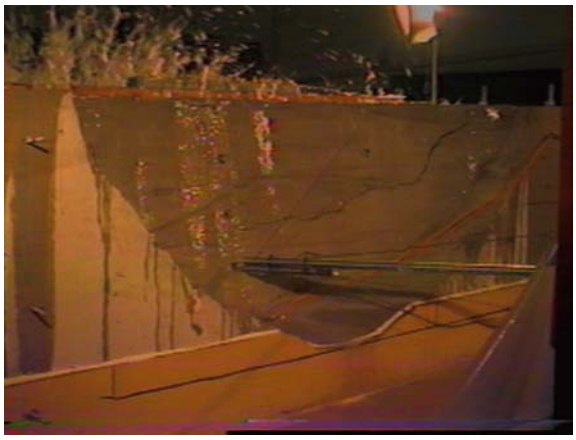

Crack Opens

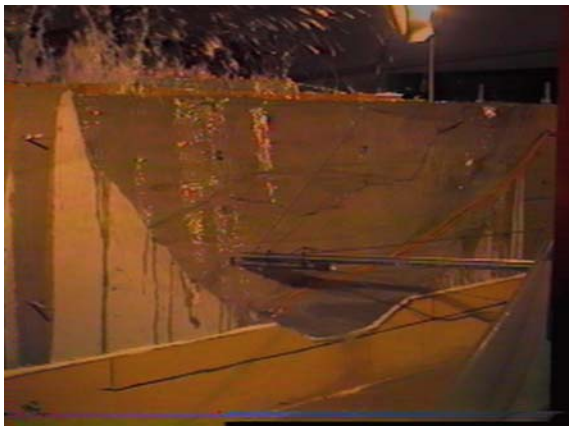

Crack Closes

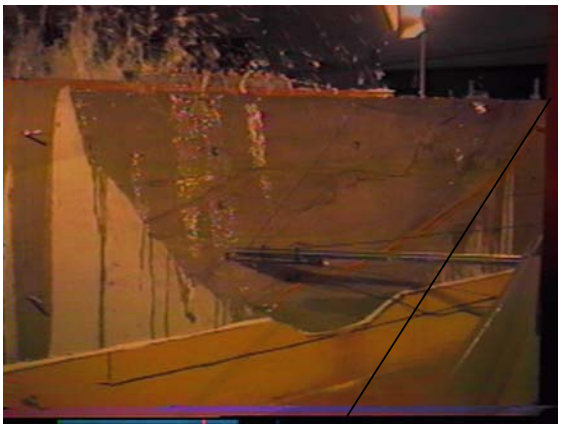

Crack Releases Water

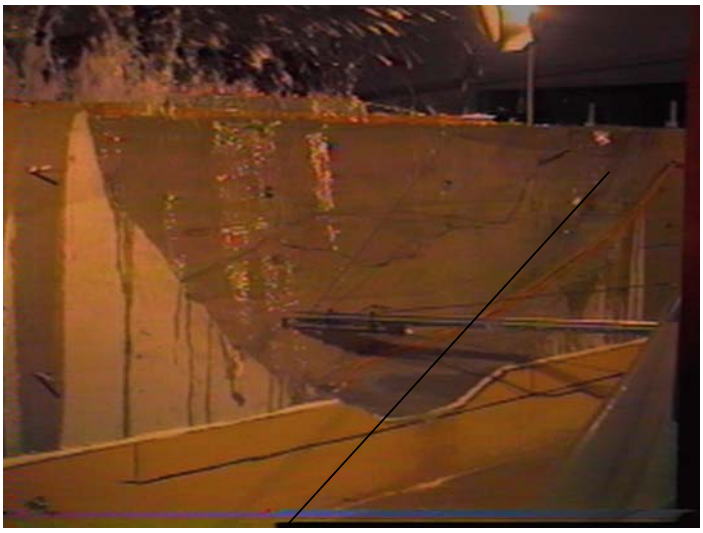

Crack Releases Water At Next Opening

Figure 36.—Sequence showing water release.

Conclusions

1. The Koyna Model gave similar results to previous studies and to what actually happened in the field. The 3-D arch dam model compares with previous models and linear measurements such as response frequencies made in the field.

2. All models show the onset of sudden cracking and pronounced structural nonlinearity following cracking. This nonlinearity is characterized by the bottom of the dam slipping back and forth beneath the top of the dam.

3. The arch dam model demonstrates a critical acceleration of 0.70 g for first cracking of this specific model.

4. The crack pattern in the models is dominated by the joint patterns.

5. The time to final full failure, when converted to full scale times, exceeds the duration of any recorded earthquake.

6. Final failure is a push through of the dam into downstream. This failure mechanism appears to require abrasion in the joint before it can be established.

7. Water passes through cracks in the model in approximately 1/10th of a second.

Recommendations

1. Physical models can be used to find extreme cases needed for the evaluation of critical structures. The results should be used to improve understanding of numerical modeling or to develop and improve capability. The results should be used to develop initial and terminal failure modes for issues such as risk analyses.

2. Some necessary data for nonlinear modeling have been gathered using preliminary testing methods. Additional work should be performed to establish methods to find necessary parameters.

3. Wide canyon dams are clearly affected by the cross-canyon mode shapes. Some studies should be conducted for narrow canyons to investigate the initiation of cracking and failure mechanisms.

References

1. Chopra, A.K., and P. Chakrabarti. 1971. *The Koyna Earthquake of December 11,1967 and the Performance of Koyna Dam.* Report No. EERC 71-1, Earthquake Engineering Center, University of California, Berkeley, California.

2. Donlon, W.P., and J.F. Hall. 1991. "Shaking Table Study of Concrete Gravity Dam Monoliths." *Earthquake Engineering and Structural Dynamics*, vol. 20, 769-786.

3. Niwa, A., and R.W. Clough. 1980. *Shaking Table Research On Concrete Dam Models*. Report No. UCB/EERC 80-05, Earthquake Engineering Research Center, University of California, Berkeley, California.

4. Norman, C.D. 1986. *Dynamic Failure Tests and Analysis of a Model Concrete Dam*. Technical Report SL-86-33, U.S. Army Waterways Experiment Station, Vicksburg, Michigan.

5. Tinawi, R., P. Leger, M. Leclerc, and G. Cipolla. September 1998. "Shake Table Tests for the Seismic Response of Concrete Gravity Dams." Eleventh European Conference on Earthquake Engineering, Paris, France.

6. Plizzari, Saouma, and Waggoner. October 1995. "Centrifuge Modeling and Analysis of Concrete Gravity Dams," *Journal of Structural Engineering*, vol. 121, No. 10, pp. 1471-1479.

7. Renzi, Ferrara, and Mazza. 1994. "Cracking In a Concrete Gravity Dam: A Centrifugal Investigation," International Workshop on Dam Fracture and Damage, Chambery, France.

8. Krawinkler, H., and P.D. Moncarz. "Similitude Requirements for Dynamic Models." American Concrete Institute, v SP-73.

9. Donlon, W.P. 1989. *Experimental Investigation of the Nonlinear Seismic Response of Concrete Gravity Dams*. Report No. EERL 89-01, Earthquake Engineering Research Laboratory, California Institute of Technology, Pasadena, 1989.

10. McCafferty, R.M. December 1970. "Test Facilities USBR Vibration Test System," *Shock and Vibration Bulletin*, Bulletin 41, pp. 109-117.

11. Niwa, A., and R.W. Clough. September 1980. *Shaking Table Research on Concrete Dam Models*. Report No. UCB/EERC 80/05.

12. Niwa, A., and R.W. Clough. 1982. "Non-Linear Seismic Response of Arch Dams." *Earthquake Engineering and Structural Dynamics,* vol. 10, 267-281.

13. Oberti, G., and A. Castoldi. 1981. "The Use of Models In Assessing the Behavior of Concrete Dams." Dams and Earthquakes - Proceedings of a conference held at the Institution of Civil Engineers, London on October 1-2, 1980, Thomas Telford Limited, London.

14. Mir, R.A., and C.A. Taylor. 1996. "An Investigation Into Base Sliding Response of Rigid Concrete Gravity Dams to Dynamic Loading." *Earthquake Engineering and Structural Dynamics*, vol. 25, pp. 79-98.

15. Yoshida, T., and K. Baba. 1965. "Dynamic Response of Dams." Proceedings of the 3rd World Conference in Earthquake Engineering, Auckland, vol. 2, pp. 748-764.

16. Oberti, G., and A. Castoldi. 1980. "The Use of Models In Assessing the Behavior of Concrete Dams." Dams and Earthquake: Proceedings of a Conference held at the Institution of Civil Engineers, London, October 1-2.

17. Oberti, G., and E. Lauletta. 1967. "Structural Models for the Study of Dam Earthquake Resistance." Ninth International Congress on Large Dams, Istanbul, Turkey, September 4-8.

18. Harris, David W., C.E. Mohorovic, and T.P. Dolen. 2000. "Dynamic Properties of Mass Concrete Obtained From Dam Cones." *ACI Materials Journal,* vol. 97, No. 3, American Concrete Institute.

19. Harris, David W., Nathan Snorteland, Timothy Dolen, and Fred Travers. 2000. "Shaking Table 2-D Models of a Concrete Gravity Dam." *Earthquake Engineering and Structural Dynamics 2000*; 29: pp. 769-787.

20. Takahashi, T. "Results of Vibration Tests and Earthquake Observations On Concrete Dams and Their Considerations." ICOLD Congress No. 8, EDINBURGH, volume II, report 14, pp. 239-260.

21. Rouse, George C., and Jack G. Bouwkamp. 1967. *Vibration Studies of Monticello Dam.* Research Report No.9, Water Resources Technical Publication, United States Department of the Interior.

22. Duron, Z.H., and J.F. Hall. 1988. "Experimental and Finite Element Studies of the Forced Vibration Response of Morrow Point Dam." *Earthquake Engineering and Structural Dynamics*, vol. 16.

23. Oberti, G.,and A. Castoldi. 1981. "The Use of Models In Assessing the Behavior of Concrete Dams." Dams and Earthquakes - Proceedings of a conference held at the Institution of Civil Engineers, London on October 1-2, 1980, Thomas Telford Limited, London.

24. Houqun, Chen, et al. July 1994. *Model Test and Program Verification on Dynamic Behavior of Arch Dams With Contraction Joints*. Institute of Water Conservancy and Hydroelectric Power Research, Report No. SVL-94/02.

25. Bureau of Reclamation. 1967. *Vibration Studies of Monticello Dam*. A Water Resources Technical Publication, Research Report No. 9, United States Department of Interior.

MISSION STATEMENTS

The Mission of the Department of the Interior is to protect and provide access to our Nation's natural and cultural heritage and honor our trust responsibilities to tribes.

The mission of the Bureau of Reclamation is to manage, develop, and protect water and related resources in an environmentally and economically sound manner in the interest of the American public.